

Journal Pre-proof

Multi-electrode stimulation evokes consistent spatial patterns of phosphenes and improves phosphene mapping in blind subjects

Denise Oswald, William Bosking, Ping Sun, Sameer A. Sheth, Soroush Niketeghad, Michelle Armenta Salas, Uday Patel, Robert Greenberg, Jessy Dorn, Nader Pouratian, Michael Beauchamp, Daniel Yoshor

PII: S1935-861X(21)00226-6

DOI: <https://doi.org/10.1016/j.brs.2021.08.024>

Reference: BRS 2046

To appear in: *Brain Stimulation*

Received Date: 17 January 2021

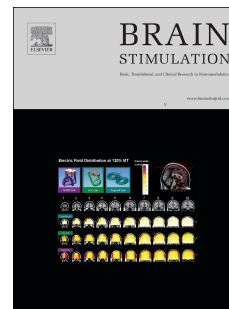
Revised Date: 11 August 2021

Accepted Date: 31 August 2021

Please cite this article as: Oswald D, Bosking W, Sun P, Sheth SA, Niketeghad S, Salas MA, Patel U, Greenberg R, Dorn J, Pouratian N, Beauchamp M, Yoshor D, Multi-electrode stimulation evokes consistent spatial patterns of phosphenes and improves phosphene mapping in blind subjects, *Brain Stimulation* (2021), doi: <https://doi.org/10.1016/j.brs.2021.08.024>.

This is a PDF file of an article that has undergone enhancements after acceptance, such as the addition of a cover page and metadata, and formatting for readability, but it is not yet the definitive version of record. This version will undergo additional copyediting, typesetting and review before it is published in its final form, but we are providing this version to give early visibility of the article. Please note that, during the production process, errors may be discovered which could affect the content, and all legal disclaimers that apply to the journal pertain.

© 2021 Published by Elsevier Inc.



Denise Oswalt: Conceptualization, Investigation, Software, Formal analysis, Visualization, Data curation, Writing – Original draft preparation. **William Bosking:** Conceptualization, Investigation, Writing – Review and editing. **Ping Sun:** Conceptualization, Investigation, Data curation, Software. **Sameer A. Sheth:** Resources, Writing – Review and editing. **Soroush Niketeghad:** Investigation, Data curation, Writing – Review and editing. **Michelle Armenta Salas:** Investigation, Writing – Review and editing. **Uday Patel:** Investigation, Software. **Robert Greenberg:** Funding acquisition. **Jessy Dorn:** Funding acquisition. **Nader Pouratian:** Funding acquisition, Resources, Writing – Review and editing. **Michael Beauchamp:** Funding acquisition, Visualization, Writing – Review and editing. **Daniel Yoshor:** Supervision, Resources, Project administration, Funding acquisition, Writing – Review and editing.

Journal Pre-proof

1
2
3
4
5
6
7
8
9
10
11
12
13
14
15
16
17
18
19
20
21
22
23
24
25

Multi-electrode stimulation evokes consistent spatial patterns of phosphenes and improves phosphene mapping in blind subjects

Denise Oswald ^a, William Bosking ^a, Ping Sun ^b, Sameer A. Sheth ^b, Soroush Niketeghad ^c, Michelle Armenta Salas ^{c,d}, Uday Patel ^d, Robert Greenberg ^d, Jessy Dorn ^d, Nader Pouratian ^{c,d}, Michael Beauchamp ^{a,b}, Daniel Yoshor ^a

^a *Department of Neurosurgery, University of Pennsylvania, PA, Philadelphia*
^b *Department of Neurosurgery, Baylor College of Medicine, TX, Houston*
^c *Department of Neurosurgery, University of California Los Angeles, CA, Los Angeles*
^d *Second Sight Medical Products, CA, Sylmar*

Corresponding Author

Denise Oswald, PhD
Perelman School of Medicine, Department of Neurosurgery
3700 Hamilton Walk, Richards 6A
Philadelphia, PA 19104
Telephone: (480)457-9553
Email: denise.oswalt@penmedicine.upenn.edu

26 **Abstract**

27

28 Background: Visual cortical prostheses (VCPs) have the potential to restore visual function to patients
29 with acquired blindness. Successful implementation of VCPs requires the ability to reliably map the
30 location of the phosphene produced by stimulation of each implanted electrode.

31

32 Objective: To evaluate the efficacy of different approaches to phosphene mapping and propose simple
33 improvements to mapping strategy.

34

35 Methods: We stimulated electrodes implanted in the visual cortex of five blind and fifteen sighted
36 patients. We tested two fixation strategies, unimanual fixation, where subjects placed a single index finger
37 on a tactile fixation point and bimanual fixation, where subjects overlaid their right index finger over their
38 left on the tactile point. In addition, we compared absolute mapping in which a single electrode was
39 stimulated on each trial, and relative mapping with sequences containing stimulation of three to five
40 phosphenes on each trial. Trial-to-trial variability present in relative mapping sequences was quantified.

41

42 Results: Phosphene mapping was less precise in blind subjects than in sighted subjects (2DRMS, $16 \pm 2.9^\circ$
43 vs. $1.9 \pm 0.93^\circ$; $t(18) = 18$, $p < 0.001$). Within blind subjects, bimanual fixation resulted in more
44 consistent phosphene localization than unimanual fixation (BS1: $4.0 \pm 2.6^\circ$ vs. $19 \pm 4.7^\circ$, $t(79) = 24$, p
45 < 0.001 ; BS2 $4.1 \pm 2.0^\circ$ vs. $12 \pm 2.7^\circ$, $t(65) = 19$, $p < 0.001$). Multi-point relative mapping had similar
46 baseline precision to absolute mapping (BS1: $4.7 \pm 2.6^\circ$ vs. $3.9 \pm 2.0^\circ$; BS2: $4.1 \pm 2.0^\circ$ vs. $3.2 \pm 1.1^\circ$) but
47 improved significantly when trial-to-trial translational variability was removed. Although multi-point
48 mapping methods did reveal more of the functional organization expected in early visual cortex, subjects
49 tended to artificially regularize the spacing between phosphenes. We attempt to address this issue by
50 fitting a standard logarithmic map to relative multi-point sequences.

51

52 Conclusions: Relative mapping methods, combined with bimanual fixation, resulted in the most precise
53 estimates of phosphene organization. These techniques, combined with use of a standard logarithmic
54 model of visual cortex, may provide a practical way to improve the implementation of a VCP.

55

56

57 **Introduction**

58

59 Technological advances have revived interest in prosthetic approaches to treat acquired blindness. In
60 recent years, several groups have brought visual cortical prostheses (VCPs) to the late development stage
61 or to actual clinical trials [1]–[3], as reviewed by [4]–[7]. VCPs consist of a camera that captures images
62 of the world, a processing module that translates images into stimulation patterns, and a set of electrodes
63 implanted in or on visual cortex. This approach bypasses damage to early visual structures such as the
64 retina or optic nerve, to deliver information directly to the brain. The basis for VCPs is built on two
65 observations: firstly, electrical stimulation of single electrodes in early visual cortex produces a visual
66 percept, or phosphene, in a discrete part of visual space [8]–[12], and secondly, visual cortex contains a
67 retinotopic map of the world [13]–[18]. In theory, multiple electrodes in early visual cortex could be
68 stimulated in precise spatiotemporal patterns to evoke the perception of specific visual forms or the entire
69 visual scene.

70

71 There are several requirements that need to be met for VCPs to be able to provide useful information to
72 users. Firstly, electrical stimulation of visual cortex must still produce visual sensations after loss of sight.
73 Evidence suggests that, while there may be some changes to cortical excitability, even patients with long-
74 standing acquired blindness can still perceive phosphenes [9], [11], [19], [12], [20], [21] as long as their
75 visual cortex is undamaged. Secondly, a structured map of visual space also needs to remain intact. While
76 cortical plasticity following long-term deafferentation may change the size of cortical areas due to
77 functional repurposing [22]–[27], previous studies indicate that the map of visual space persists in cortex

78 years after loss of sight [11], [12], [21]. In addition to these biological requirements, to successfully
79 deploy a VCP requires methods that are reliable and efficient at phosphene mapping [9], [28], [19], the
80 process of determining the location of the phosphene generated by electrical stimulation of the implanted
81 electrodes.

82
83 In practice, phosphene mapping has been reproached in two ways, absolute and relative [9], [29]. For
84 absolute mapping, the subject reports the location of a single phosphene relative to a central fixation
85 point. For relative mapping, the subject reports the spatial relationship between phosphenes (relative
86 angle and distance). In sighted subjects, phosphene mapping is typically conducted with an absolute
87 approach and is a straightforward process. Subjects visually fixate on a monitor placed in front of them,
88 and after electrical stimulation is delivered to an electrode, they make visually guided movements to point
89 to or draw the location of the perceived phosphene on the monitor, with respect to the fixation point. This
90 type of phosphene mapping has been conducted in sighted epilepsy subjects, and in general has resulted
91 in determination of phosphene locations for each electrode that closely match the receptive field (RF)
92 location measured for the same electrodes [5], [30], [31].

93
94 There is good reason to expect mapping phosphene locations would be more difficult in blind subjects.
95 Without visual inputs, blind subjects are unable to take advantage of either visual fixation or visually
96 guided pointing. Rather than visual fixation, blind subjects are instructed to use one hand to maintain
97 contact with a tactile fixation point, and to report the location of an electrically evoked visual sensation
98 with their other hand [11], [12], [32], using a reaching movement, for which their only feedback is
99 proprioception of the hand fixating and the arm used for pointing. The limited tactile cues yield an
100 impoverished framework for the reporting environment and provide less feedback that could be used to
101 compensate for subtle errors that occur on each trial, which may be exaggerated in absolute mapping.
102 Both absolute and relative methods have been attempted in blind subjects. The investigators that created
103 the first prototype VCPs used both methods and reported on some of the differences between the two

104 methods [9], [11], [32], [33]. However, no systematic and quantitative investigation of the reliability of
105 the two methods has been conducted in blind subjects.

106

107 The main rationale behind use of relative mapping methods is that most of the error in phosphene
108 mapping results from small errors in gaze direction at the start of each trial. It is assumed that by
109 stimulating two or more electrodes on a single trial the relative arrangement between the phosphenes
110 associated with each electrode can be measured. However, for relative mapping to be successful it is
111 necessary that the spatial pattern or configuration of phosphenes perceived by the subject be stable across
112 trials. There are reasons to believe that spatial configurations are stable across trials and can be used to
113 guide discriminations [21], [34] but this observation and its relationship to the improvement in phosphene
114 mapping reliability have not yet been carefully examined.

115

116 In this report, we utilize data from two rare populations, sighted patients undergoing monitoring for
117 medically refractory epilepsy and blind patients implanted with an early generation VCP. We found blind
118 subjects to have significantly impoverished performance in phosphene localization relative to sighted
119 subjects. This comparison was used to demonstrate the need for mapping methods tailored specifically to
120 the blind subjects who will be the recipients of the next generation of VCPs. We approached this goal in
121 two ways. The first technique was to improve the quality of the tactile fixation with a bimanual approach,
122 using the index finger from each hand on the tactile fixation point. The second technique was to use
123 relative mapping methods (stimulating two or more electrodes per trial in sequence). Finally, we show
124 how relative mapping methods could be more effective at revealing some important features of the map of
125 visual space and propose a combination of relative mapping and a standardized logarithmic map of visual
126 space to adequately capture the organization and structure specific to each subject.

127

128 **Methods**

129

130 *Subjects*

131

132 All research and protocols were approved by Institutional Review Boards at Baylor College of Medicine
 133 (BCM) and University of California, Los Angeles (UCLA), and all subjects gave written informed
 134 consent. Data were collected from fifteen sighted and six blind subjects. Sighted subjects were patients
 135 with medically refractory epilepsy treated at BCM. Subjects were male and female, aged 22-61, with a
 136 mean age of 35. Sighted subjects were hospitalized in the epilepsy monitoring unit for 4-14 days
 137 following surgical implantation of subdural electrode grids and strips. Fifteen sighted subjects were
 138 included in this report. The original case identifiers for these subjects were LF, MR, YAA, YAB, YAC,
 139 YAE, YAF, YAH, YAI, YAM, YAN, YAO, YAU, YAV, YAX, and can be used to compare with earlier
 140 and future reports using these subjects. For ease of referral, the remainder of this report will refer to each
 141 sighted subject by a designated local identifier, SS1 through SS15, respectively.

142

143 All blind subjects are participants in an ongoing early feasibility study (NCT03344848) for the Orion
 144 visual cortical prosthesis (Second Sight Medical Inc.) being conducted at BCM and the University of
 145 California, Los Angeles. Subjects were male and female, aged 29-64, mean age 49. All subjects had
 146 usable vision in early life, and late onset blindness. Causes of blindness for each subject are summarized
 147 below in Table 1. For ease of referral in the remainder of this report each subject has been given local
 148 identifiers in addition to their clinical trial identifiers as indicated in the table below.

149

| Site | Global ID | Local ID | Age of Onset | Age at Implant | Gender | Etiology | Bare Light Perception |
|------|-----------|----------|--------------|----------------|--------|-------------|-----------------------|
| UCLA | 02-659 | BS1 | 22 | 29 | Male | Head trauma | None |
| BCM | 03-281 | BS2 | 45 | 57 | Male | Head Trauma | None |

| | | | | | | | |
|------|--------|-----|----|----|--------|-------------------------------------------|------------------------------|
| UCLA | 02-334 | BS3 | 53 | 56 | Male | Optic neuropathy secondary to burn/trauma | Minimal in contralateral eye |
| UCLA | 02-941 | BS4 | 63 | 64 | Female | Retina damage secondary to liver abscess | None |
| UCLA | 02-182 | BS5 | 20 | 52 | Male | Congenital Glaucoma | None |

150

151 Table 1. Blind subject information. Table indicates subject global and local identifiers, study site, age at
 152 time of implant, age of onset of blindness, and cause of blindness.

153

154 *Electrodes and Electrical Stimulation*

155

156 Sighted subjects were implanted with subdural grids and strips with standard clinical electrodes (3mm
 157 diameter) for monitoring of epileptogenic activity. Placement of electrodes in these subjects was guided
 158 by clinical criteria. In most sighted subjects, select implanted subdural strips also contained additional
 159 research mini electrodes (0.5 mm diameter) imbedded in between the larger clinical contacts (SS3 –
 160 SS15), two subjects (SS1 and SS2) had grids containing only the standard clinical electrodes implanted.
 161 Research strips were one of three configurations. Schematics of each array configuration implanted in
 162 each sighted subject are available in Table S1.

163

164 Clinical and research grids and strips were manufactured by PMT (Chanhassen, MN). Electrical
 165 stimulation was performed with a 16-channel AlphaLab SnR (Alpha Omega, Alpharetta, GA) and
 166 controlled by a custom user interface developed in MATLAB (Version 2013b, The MathWorks Inc,
 167 Natick, MA). All stimulation was monopolar, grounded to a return pad placed on the subject's thigh.
 168 Stimulation was comprised of pulse trains 200 ms in duration composed of biphasic 0.1 ms per phase,
 169 square, symmetric pulses, delivered at 200 Hz.

170

171 Blind subjects were each implanted with the Orion Visual Cortical Prosthesis System (Second Sight
172 Medical Products Inc, Sylmar CA). The implanted system consists of an array of 60 electrodes, 2 mm in
173 diameter, spaced 3 mm apart diagonally and 4.2 mm apart within rows, center-to-center (Figure 1C), and
174 an internal processing control module imbedded in the skull. Each 2 mm electrode consisted of an
175 electrically contiguous group of thirty-seven 0.2 mm diameter circular contacts, made from sputtered
176 platinum gray on silicone. The implanted processing module delivers electrical stimulation and acts as the
177 return for monopolar stimulation. Electrical stimulation was controlled via a software interface developed
178 by Second Sight Medical Products. Stimulation consisted of 100-250 ms duration pulse trains composed
179 of biphasic 0.2 ms per phase, square, symmetric pulses, delivered at 20, 60, or 120 Hz. Pulse duration
180 used was the standardized value used across the clinical trial. Pulse frequency increments and maximum
181 value were limited by the hardware capabilities of the Orion Visual Processing Unit (VPU). Stimulation
182 implemented with BS1 was conducted at 60 Hz at the request of the clinical trial sponsor for the safety of
183 this subject. Stimulation carried out with BS2 was conducted at 120 Hz. A summary of stimulation
184 parameters specific to each task is available below in Table 2.

185

186 *Electrode localization*

187

188 Pre- and post-surgical imaging was used to determine electrode locations for each subject. Prior to
189 surgery, subjects underwent T1-weighted structural MRI in a 3T scanner. These scans were used to create
190 cortical surface models using FreeSurfer [35], [36]. Whole-head CT was conducted post-implant and
191 aligned to pre-surgical imaging using Analysis of Functional Neuroimaging (AFNI) software [37].
192 Electrode locations were manually determined using a combination of AFNI and SUMA [38] and
193 projected to the nearest node of the cortical surface model using custom methods developed in MATLAB
194 (Version 2019a, The MathWorks Inc, Natick, MA).

195

196 *Screening and threshold determination*

197

198 Screening sessions were conducted to determine which electrodes reliably produced phosphenes when
199 electrically stimulated and to determine the current amplitude at which each subject could reliably
200 perceive and localize a phosphene. For sighted subjects, screening trials consisted of an auditory cue
201 followed by electrical stimulation and a verbal report by the subject of whether stimulation evoked a
202 percept. The current amplitude was stepped from 0.3-4.0 mA, until the subject reported a phosphene.
203 Electrodes that did not evoke a phosphene at 4.0 mA were excluded. For the phosphene mapping
204 experiments reported here, the current used for testing was selected to be above threshold such that
205 stimulation always produced a phosphene that was easy to perceive and localize on every trial.

206

207 For blind subjects, electrodes with impedance above 18 k Ω were disabled. Initial viability and thresholds
208 for each electrode was determined using a staircase threshold procedure set by the clinical trial sponsor.
209 Electrical stimulation was applied at currents incremented from 0 to 8 mA, with three repeats at each
210 increment. Threshold was determined as the lowest current for which three consecutive trials produced a
211 phosphene. Currents used during comparative mapping tasks were secondarily adjusted by incrementing
212 the current amplitude delivered to each electrode until the subject could easily perceive and localize each
213 phosphene. Qualitative adjustments were made to equalize the subjective brightness and size of each
214 phosphene perceived.

215

216 *Fixation techniques*

217

218 Sighted subjects were instructed to visually fixate on a 0.5° cross presented on the monitor by training
219 their gaze and focusing their attention on this point. On each trial, subjects were asked to maintain

220 fixation from before the onset of electrical stimulation until they had completed their report of phosphene
221 location on the touchscreen.

222

223 Blind subjects were instructed to fixate on a tactile point placed on the touchscreen monitor. They were
224 asked to focus their attention on the tactile point at the tip of their finger(s) and to imagine looking toward
225 this point. If they retained an eye(s), they were asked to keep their eyes still and pointed toward the tactile
226 point to the best of their abilities. Two forms of tactile fixation were evaluated in blind subjects,
227 unimanual and bimanual. For unimanual fixation subjects were instructed to place their left index finger
228 on a tactile point approximately 0.5° in diameter that was placed on the monitor, and to direct their
229 attention toward that digit (Figure 2A, upper). Following stimulation, the subject used their right index
230 finger to indicate phosphene location, while maintaining fixation on their left index finger. This fixation
231 protocol was used for the initial comparison of phosphene variability between sighted and blind subjects.
232 For bimanual fixation, subjects were instructed to place their left index finger on the tactile point and to
233 overlay their right index atop their left, and then focus their attention on both fingertips (Figure 2A,
234 lower). The subject reported phosphene location with their right index finger, while maintaining attention
235 on the fixation point. This protocol was used for the comparison between absolute and multi-point relative
236 mapping strategies.

237

238 *Phosphene mapping strategies*

239

240 We compared two phosphene mapping techniques, absolute and multi-point relative. Absolute mapping
241 was conducted in all sighted and blind participants, multi-point mapping was evaluated only in blind
242 subjects BS1 and BS2. The stimulation parameters used with each subject and each task are summarized
243 later in Table 2.

244

245 *Absolute mapping*

246

247 Sighted subjects were seated comfortably in front of a touchscreen monitor (Wacom, Toyonodai, Kazo-
248 shi, Saitama, Japan) placed 28.6 to 57.3 cm in front of them and instructed to visually fixate (Figure 1B).
249 Monitor distance was adjusted to the allow receptive fields of the electrodes tested to fit on the monitor
250 screen. On each trial, electrical stimulation was delivered to a single electrode, followed by an audible
251 cue, and then subject response (Figure 1A). Size, shape, and location of the phosphene were reported by
252 the subject drawing the percept on the monitor.

253

254 Blind subjects were seated 30.5 cm in front of a touchscreen monitor and instructed to fixate on a tactile
255 point (Figure 1D). At this distance, the monitor encompasses a range of 50° by 45°. This distance was set
256 by the clinical trial because it provided touch screen dimension which fully encompassed the expected
257 range of visual field coverage of the implanted array and was found to be a comfortable distance for
258 subjects to report. Electrical stimulation was delivered to one electrode per trial, after which subjects were
259 instructed to report with their right index finger the location of the center of the perceived phosphene, or
260 to draw the outline of the perceived phosphene in the location where it was perceived. Out of the 60
261 electrodes implanted, 50 – 59 electrodes were mapped per subject. Bimanual absolute mapping was
262 conducted at 120 Hz for BS2 (03-281), while 60 Hz was used for BS1 (02-659), at the request of the
263 clinical trial sponsor. Two blind subjects performed bimanual absolute mapping; BS1 mapped 25
264 electrodes in this setup, and BS2 mapped 46 in this setup. The comparison to unimanual fixation only
265 used the electrodes mapped with both fixation techniques.

266

267 *Relative mapping*

268

269 Multi-point mapping consisted of sequential stimulation of 3-5 electrodes. Sequential, rather than
 270 concurrent, stimulation was employed for two primary reasons. Firstly, the current threshold for
 271 perception was relatively large, and there was a safety concern to stimulate more than two electrodes at
 272 once. Secondly, with the blind subjects evaluated, stimulation delivered simultaneously on two electrodes
 273 often resulted in one phosphene in a location spatially distinct from that produced by either electrode
 274 stimulated individually. Electrode sequences stimulated a series of adjacent electrodes on the array.
 275 Generally, electrode sequences were selected so that they did not cross a major sulcus, such as the
 276 calcarine fissure, and were composed of electrodes that were all in the same cortical area (all in V1 or
 277 V2). For instance, in BS2, one sequence consisted of the first through fourth electrodes in the top row of
 278 the array (electrodes 1 – 4). Another sequence consisted of the first electrode in row 5, the second
 279 electrode in row 6, and the third electrode in row 7. In total, BS conducted 22 sequences, mapping 48
 280 electrodes across 2 sessions, and BS2 conducted 26 sequences, mapping 50 electrodes across 7 sessions,
 281
 282 On each trial, a 100 ms duration pulse train was delivered to each electrode, with a 250 ms gap between
 283 each electrode in the sequence (Figure 3A). Stimulation conducted with BS2 was delivered at 120 Hz;
 284 stimulation conducted with BS1 used 60 Hz at the request of the trial sponsor. Sequence timing was
 285 selected be short enough to reduce eye movements during the trial, but long enough that each phosphene
 286 was perceived separately. A tone presented at the end of the stimulation sequence cued subjects to
 287 respond. Subjects indicated on a touchscreen monitor the center of each phosphene in the order and
 288 location perceived (Figure 3B).

289

| Subject | Task | Fixation | Frequency (Hz) | Pulse Width (ms) | Duration (ms) |
|---------|--------------|----------|----------------|------------------|---------------|
| SS1 | Thresholding | None | 200 | 0.1 | 200 |
| SS2 | Thresholding | None | 200 | 0.1 | 200 |
| SS3 | Thresholding | None | 200 | 0.1 | 200 |
| SS4 | Thresholding | None | 200 | 0.1 | 200 |
| SS5 | Thresholding | None | 200 | 0.1 | 200 |

| | | | | | |
|------|---------------------|-----------|-----|-----|-----|
| SS6 | Thresholding | None | 200 | 0.1 | 200 |
| SS7 | Thresholding | None | 200 | 0.1 | 200 |
| SS8 | Thresholding | None | 200 | 0.1 | 200 |
| SS9 | Thresholding | None | 200 | 0.1 | 200 |
| SS10 | Thresholding | None | 200 | 0.1 | 200 |
| SS11 | Thresholding | None | 200 | 0.1 | 200 |
| SS12 | Thresholding | None | 200 | 0.1 | 200 |
| SS13 | Thresholding | None | 200 | 0.1 | 200 |
| SS14 | Thresholding | None | 200 | 0.1 | 200 |
| SS15 | Thresholding | None | 200 | 0.1 | 200 |
| BS1 | Staircase threshold | None | 20 | 0.2 | 250 |
| BS2 | Staircase threshold | None | 20 | 0.2 | 250 |
| BS3 | Staircase threshold | None | 20 | 0.2 | 250 |
| BS4 | Staircase threshold | None | 20 | 0.2 | 250 |
| BS5 | Staircase threshold | None | 20 | 0.2 | 250 |
| BS1 | Current Selection | None | 60 | 0.2 | 100 |
| BS2 | Current Selection | None | 120 | 0.2 | 100 |
| SS1 | Absolute Mapping | Visual | 200 | 0.1 | 200 |
| SS2 | Absolute Mapping | Visual | 200 | 0.1 | 200 |
| SS3 | Absolute Mapping | Visual | 200 | 0.1 | 200 |
| SS4 | Absolute Mapping | Visual | 200 | 0.1 | 200 |
| SS5 | Absolute Mapping | Visual | 200 | 0.1 | 200 |
| SS6 | Absolute Mapping | Visual | 200 | 0.1 | 200 |
| SS7 | Absolute Mapping | Visual | 200 | 0.1 | 200 |
| SS8 | Absolute Mapping | Visual | 200 | 0.1 | 200 |
| SS9 | Absolute Mapping | Visual | 200 | 0.1 | 200 |
| SS10 | Absolute Mapping | Visual | 200 | 0.1 | 200 |
| SS11 | Absolute Mapping | Visual | 200 | 0.1 | 200 |
| SS12 | Absolute Mapping | Visual | 200 | 0.1 | 200 |
| SS13 | Absolute Mapping | Visual | 200 | 0.1 | 200 |
| SS14 | Absolute Mapping | Visual | 200 | 0.1 | 200 |
| SS15 | Absolute Mapping | Visual | 200 | 0.1 | 200 |
| BS1 | Absolute Mapping | Unimanual | 60 | 0.2 | 100 |
| BS2 | Absolute Mapping | Unimanual | 120 | 0.2 | 100 |
| BS3 | Absolute Mapping | Unimanual | 20 | 0.2 | 250 |
| BS4 | Absolute Mapping | Unimanual | 20 | 0.2 | 250 |
| BS5 | Absolute Mapping | Unimanual | 20 | 0.2 | 250 |
| BS1 | Absolute Mapping | Bimanual | 60 | 0.2 | 100 |
| BS2 | Absolute Mapping | Bimanual | 120 | 0.2 | 100 |

| | | | | | |
|-----|------------------|----------|-----|-----|-----|
| BS1 | Relative Mapping | Bimanual | 60 | 0.2 | 100 |
| BS2 | Relative Mapping | Bimanual | 120 | 0.2 | 100 |

290

291 Table 2. Stimulation parameters by subject and task. Table presents stimulation parameters used during
 292 each task and each subject.

293

294 *Trial-to-trial precision*

295

296 Precision of localized phosphenes was quantified with a two times distance root mean square metric
 297 (2DRMS). This metric was calculated within-session, for each electrode mapped.

$$2DRMS = 2 \sqrt{\sigma_x^2 + \sigma_y^2}$$

298 where σ_x is the x component of the standard deviation of the point cloud, and σ_y is the y component.

299

300 *Data alignment*

301

302 No alignment was applied to absolute mapping data. Final phosphene locations for each mapped electrode
 303 were determined by averaging phosphene locations across all trials for a given electrode.

304

305 Linear transforms (translation, rotation, and scaling) were used to align relative mapping trials. Trials for
 306 each sequence were first aligned to the center of mass across all trials. The set of phosphene locations
 307 from each trial was then rotated around its center of mass until equal to the average angle across all trials.

308 Next, length of each pattern in degrees was determined by summing the length between each node, the

309 average value was determined, and each trial was scaled such that its total length matched the group

310 average. Precision following alignment was evaluated for all trials within a single session, as well as

311 evaluated across sessions for any sequences presented in multiple sessions. The magnitude of each type of
312 observed variation (translation, rotation, scaling) was evaluated within each session and across sessions.

313

314 *Contribution of each type of trial variation on imprecision*

315

316 A generalized linear model was fit to evaluate the contribution of each type of observed trial
317 variation (translation, rotation, and scale) on 2DRMS. Models were fit in MATLAB using the
318 native function *fitglm()*. A linear fit, with a normal distribution and reciprocal link was used.

319 Input values were the average translation, rotation, and scale factor for each sequence during
320 each session, and the output parameter was the average 2DRMS of each mapped phosphene in
321 each sequence. Model fits with interactions were evaluated, with no significant interactions
322 identified between each variation.

323

324 *Cortical magnification factor*

325

326 Cortical magnification factor (CMF) was used to further analyze map structure. This was calculated by
327 the ratio of distance on the surface of the brain in mm to the distance in visual space for phosphenes
328 evoked by electrical stimulation on neighboring electrodes:

$$\text{CMF} = \frac{d_{e1-e2}}{d_{p1-p2}}$$

329 where d_{e1-e2} is the center-to-center distance of electrodes 1 and 2 on the array in mm and d_{p1-p2} is the
330 distance in visual space between phosphenes evoked by electrode 1 and 2 in degrees. This was calculated
331 for each trial of multi-point mapping for pairs of phosphenes evoked by neighboring electrodes. Electrode
332 pairs evaluated were restricted to be located on the same gyrus and to lie in V1.

333

334 A standard mapping equation was used to estimate the expected relationship between CMF and
 335 eccentricity for each subject (see solid lines in Figure 8) [15], [17], [31]. The value for the scaling factor A
 336 was determined for each subject. This was done by evaluating a range of scaling factors between 15-45
 337 and using phosphene data from all sequences collected, to determine which scale factor provided the best
 338 agreement between expected and actual separation on cortex. Scaling factors were restricted to this range
 339 based on MRI evaluations of many normally sighted subjects [17].

$$\text{CMF}_{\text{mdl}} = \frac{A}{\text{ecc} + 3.67}$$

340 where CMF_{mdl} is the predicted CMF, A is the area scaling factor, and ecc is eccentricity.

341

342 *Array placement on a logarithmic map of the cortical sheet*

343

344 A flat map model of the V1-V3 complex known as the Banded Double-Sech model [39] was created for
 345 BS1 and BS2 (Figures 7 and S5). Using modified code from [39], a scale factor based on data from multi-
 346 sequence mapped phosphenes was used to adjust the model for each subject. Once the scaling parameter
 347 was determined, phosphenes obtained from each multi-electrode sequence tested were projected on to the
 348 flat map based on their location in visual space. The electrode array was assumed to be rigid and to lie flat
 349 on the cortical surface. The location and rotation of the electrode array on the flat map model was
 350 determined for each subject by implementing a cost function to minimize the sum of a weighted distance
 351 between the projected cortical location of each phosphene from each sequence and the electrode that
 352 evoked it. Projection of phosphene locations to cortical space from visual space was conducted using
 353 functions provided by [39]. The cost function applied was:

$$D(x, y, \theta) = \sum_1^p W_p * \sqrt{(x_p - x_e)^2 + (y_p - y_e)^2}$$

$$W_p = \frac{n_t}{2\text{DRMS}_p}$$

354 where D is the value to minimize, x and y are cartesian coordinates in brain space, θ is the angle of
355 rotation applied to the grid segment, x_p and y_p are the coordinates of each individual phosphene evoked
356 during multi-point mapping that have been projected into cortical space, x_e and y_e are the coordinates of
357 the electrode which evoked that phosphene, and W_p is a weight parameter determined by the number of
358 trials (n_t) a certain sequence was repeated across all sessions during which that sequence was mapped,
359 divided by the precision of that phosphene as measured by 2DRMS.

360
361 Fitting was conducted separately for contiguous groups of electrodes that lay on either side of the
362 calcarine. Groups were additionally divided into separate groups per visual area (V1 and V2) on either
363 side of the calcarine fissure. This resulted in three individually placed segments per subject (BS1: V1
364 upper field, V1 lower field, V2 upper field; BS2: V1 upper field, V1 lower field, V2 lower field). Once
365 the best location for each portion of the electrode array was determined on the flat map model, the model
366 was used to project the electrode coordinates from cortical space to a phosphene prediction in visual
367 space.

368

369

370 Results

371

372 *Reliability of phosphene reporting in sighted and blind subjects*

373

374 We first conducted a direct comparison of trial-to-trial precision of reported phosphene location with
375 absolute mapping between sighted and blind participants. Sighted subjects used a visual fixation point
376 (Figure 1B) during electrical stimulation, and the blind subjects used unimanual tactile fixation (Figure
377 1D). Precision of phosphene location was quantified by 2DRMS and calculated for each electrode
378 mapped. Precision of reported phosphene locations among blind participants were substantially poorer

379 than among sighted participants (Figure 1E-F; 2DRMS mean \pm standard deviation, $16\pm 2.9^\circ$ vs. $1.9\pm 0.93^\circ$;
380 $t(18) = 18$, $p < 0.001$).

381

382 This comparison between the precision of phosphene mapping in sighted and blind subjects, using
383 standard techniques used in the two populations, was made to illustrate the magnitude of the challenge
384 faced in conducting future phosphene mapping in blind VCP recipients. The rest of our report will focus
385 on how to improve the precision of phosphene mapping specifically within the blind population.

386

387 *Improvement in reliability based on fixation method*

388

389 Next, we evaluated whether a different fixation method could improve precision of phosphene location
390 among blind participants. In this fixation technique, which we refer to as bimanual fixation, subjects were
391 instructed to use both left and right index fingers on the tactile fixation point during stimulation, and then
392 report phosphene location using their right index finger while maintaining left index finger contact with
393 the fixation point (Figure 2A). The precision of phosphene reporting with bimanual fixation was
394 significantly better than with unimanual fixation (Figure 2B; BS1: $4.7\pm 2.6^\circ$ vs. $19\pm 4.4^\circ$, $t(79) = 7$, p
395 < 0.001 ; BS2 $4.1\pm 2.0^\circ$ vs. $12\pm 2.4^\circ$, $t(65) = 7$, $p < 0.001$).

396

397 *Improvements in precision based on mapping method*

398

399 Having established that bimanual fixation led to improved precision in phosphene reporting, we next
400 assessed whether relative mapping (Figure 3A-B) could further enhance reliability. Provided that a stable
401 spatial pattern or configuration of phosphenes results from each trial of electrical stimulation, relative
402 mapping using multiple electrodes could lead to better estimates of the location of the phosphenes for

403 each electrode in the sequence after small errors in absolute location, size, and angle of the perceived
404 pattern are subtracted out. We found this to be the case in our blind subjects.

405
406 Without removing the trial-to-trial errors in overall location, angle, and size of perceived patterns,
407 phosphene reporting precision as measured by 2DRMS for each electrode was similar across absolute
408 (Figure 2B), and multi-point relative (Figure 3C *raw*) mapping methods (BS1: $4.7 \pm 2.6^\circ$ vs. $3.9 \pm 2.0^\circ$; BS2:
409 $4.1 \pm 2.0^\circ$ vs. $3.2 \pm 1.1^\circ$).

410
411 Next, we examined the precision of phosphene reporting following removal of the three most prominent
412 types of trial-to-trial variation observed, global changes in translational, rotational, and scaling (Figure
413 3C). Removal of translational deviations significantly improved the precision of phosphene reporting with
414 multi-point sequences compared to the raw trials (BS1: $1.6 \pm 1.3^\circ$ vs. $3.9 \pm 2.0^\circ$ ($p < 0.001$); BS2: $1.3 \pm 0.84^\circ$
415 vs. $3.2 \pm 1.1^\circ$ ($p < 0.001$)) and represented the largest contribution to imprecision across the three types of
416 errors described. Removing rotational variation further improved precision (smaller 2DRMS) for
417 phosphene location for both BS1 and BS2 for multi-point sequences (BS1: $1.5 \pm 0.27^\circ$; BS2: $1.1 \pm 0.50^\circ$).
418 The small improvement over removal of translational shifts was significant for BS2 ($p < 0.001$).
419 Additionally, removing scaling variation from multi-point sequences resulted in a small, but significant
420 improvement in precision for BS2 ($0.84 \pm 0.41^\circ$, $p < 0.001$), but not BS1 ($0.99 \pm 0.95^\circ$, $p < 0.1$).

421
422 *Quantification of variability in relative mapping*

423
424 We next quantified the magnitude and full range of the types of trial-to-trial variability observed in multi-
425 point mapping. The mean displacement of the reported location of a phosphene sequence was less than 2°
426 from the average reported location of all trials for a given multi-point sequence (Figure 3D, dashed lines;
427 BS1: $1.5 \pm 0.69^\circ$; BS2: $1.2 \pm 0.34^\circ$). Across all trials of all sequences collected, the maximum amount of
428 shift (Figure 3D) of a single sequence's reported location from the average location was several degrees

429 in magnitude (BS1: 7.1°; BS2: 5.2 °). The mean rotation across all trials and sequences (Figure 3E, dashed
430 lines) was similar for both subjects (BS1: 5.1±6.5°; BS2: 9.1±13°). Although mean perceived and reported
431 rotation of a sequence was low, the maximum rotation of a sequence from its mean orientation observed
432 was much larger for both subjects (BS1: 68°; BS2: 89°). Average changes in the scaling or size of the
433 perceived patterns (Figure 3F, dashed lines) obtained with multi-point stimulation were generally less
434 notable than either translational or rotational variations (BS1: 1.0±0.14; BS2: 1.0±0.15), with similar
435 range of deviations for both BS1 and BS2 (BS1: 0.62 – 1.8; BS2: 0.49 – 1.8).

436

437 A generalized linear model was used to formally evaluate the impact of each source of trial variation
438 identified on the precision metric (2DRMS). A linear model with normal distribution and reciprocal
439 linkage was used. In the case of each subject, translation was found to be the most significant (BS1: $p =$
440 $4.0e-8$; BS2: $p = 0.0058$), followed by rotation (BS1: $p = 0.029$; BS2: $p = 0.035$). Scale was not
441 significantly represented in the model for either subject. Interactions were not found to be significant
442 between any of the three parameters.

443

444 *Examples of trial-to-trial variation present in specific multi-point sequences*

445

446 Two examples from BS2 are presented to demonstrate the type and range of errors that occur across trials
447 when a phosphene sequence is presented to a blind subject via electrical stimulation of early visual cortex
448 (Figure 4). The first example sequence (Figure 4A-D) was presented eleven times during a single session,
449 where trials were presented intermixed with other multi-point sequences. The subject indicated each
450 phosphene was spatially and temporally distinct, with each individual phosphene clearly visible and each
451 appearing at a similar brightness. Raw trials (Figure 4A) indicate a substantial variability in the absolute
452 location, angular orientation, and scale of the perceived pattern of phosphenes. Translational deviation
453 accounts for a large portion of the trial-to-trial variability, and once removed, a more consistent pattern
454 emerges (Figure 4B). Removing angular variation further reveals a consistent shape (Figure 4C). Finally,

455 after removing trial-to-trial variation in scaling, the spatial configuration observed across trials was
456 robustly repeated and internally consistent (Figure 4D). A second example of trial-trial variation in
457 reporting of patterns, shows a sequence that evokes phosphenes in the pattern of a simple character
458 (Figure 4E-H). As with the first example, removing trial-to-trial errors in translation (Figure 4F), rotation
459 (Figure 4G), and scaling (Figure 4H) reveals that the subject very reliably perceived a consistent spatial
460 pattern of phosphenes.

461

462

463 *Examples of variability in pattern across sessions*

464

465 Having documented the range of trial-to-trial variation in phosphene reporting observed within single
466 reporting sessions, we now present two examples illustrating the variability in perceived phosphene
467 patterns across sessions (Figure 5). The first example (Figure 5A-C) shows the phosphene pattern
468 resulting from electrical stimulation on the same exact sequence of electrodes presented during six testing
469 sessions conducted on different days. The full set of trials from all sessions show the center of the
470 phosphene pattern varies in location from a minimum elevation of -0.75° to a maximum of 6.8° , and a
471 minimum azimuth of 3.4° to a maximum of 9.0° , with an average total length of 7.3° (Figure 5A). The
472 range of variation in rotation of the perceived patterns across all trials is $\pm 5.7^\circ$ from the average
473 orientation. When trials were aligned within sessions (Figure 5B), trials from different sessions tend to
474 cluster in slightly displaced parts of visual space, with some variation in orientation and scaling of the
475 perceived pattern. Trials aligned across sessions (Figure 5C) reflect a clear and robust spatial pattern, with
476 consistent relative angles and spacing between phosphenes. A second example shows phosphenes
477 resulting from partially overlapping sequences of electrodes from five different sessions with a minimum
478 of three overlapping electrodes (Figure 5D-F). When we examine the full set of trials across all sessions,
479 (Figure 5D), the electrodes common to the tested sequences (38, 39, and 40), evoked phosphenes centered

480 across a wide range of visual space locations (AZ: $-0.10^\circ - 5.9^\circ$; EL: $-18^\circ - -7.2^\circ$), and generally
481 separated into distinct spatial regions when aligned within sessions (Figure 5E). Following alignment
482 across sessions using the common electrodes mapped, the spatial configuration of the phosphenes
483 obtained on each trial was again revealed to be consistent across sessions (Figure 5E).

484

485 When presenting the same sequence of electrodes (38-39-40) as part of a larger sequence, the subject
486 reported a consistent configuration among these electrodes but incongruous spatial relationships among
487 the remaining portions of the sequence (Figure 5F). Each series resulted in the same configuration of the
488 final three phosphenes, despite having different starting points. The electrodes that were not in common
489 across all sessions, however, had more variability in their reported location. Sequences presented in
490 session 1 (S1) and session 2 (S2), despite presenting phosphenes evoked from overlapping electrodes,
491 result in different reported configurations when one electrode was omitted from the series, which can be
492 seen in the fanning-out of sequence outside of the phosphenes evoked by electrodes 38, 39, and 40.

493

494 *Quantification of pattern variability across sessions*

495

496 The above examples show that spatial configurations of phosphenes obtained with multi-point relative
497 mapping remain stable within and across sessions. We next compared the precision of phosphene
498 mapping and magnitude of trial variation within and across sessions (Figure 6). In general, precision of
499 reported phosphene location measured across multiple sessions was lower for absolute mapping than
500 multi-point relative mapping (Figure 6B, first and third datasets presented, BS2: $6.5 \pm 1.2^\circ$ vs. 4.7 ± 1.1).
501 When examining all multi-point trials across sessions without alignment, as compared to only examining
502 trials within single sessions, there was a higher magnitude of translational, rotational, and scaling errors
503 (Figure 6, BS2: F-H) and lower precision for trials (Figure 6B, middle two columns, BS2: $4.7 \pm 1.1^\circ$ vs.
504 $3.6 \pm 1.3^\circ$). However, once trials were aligned, the precision of phosphene locations is similar for trials

505 aligned within a single session compared to trials aligned across multiple sessions (Figure 6B, right two
506 columns, BS2: $0.80 \pm 0.32^\circ$ vs. $0.91 \pm 0.25^\circ$). This provides strong evidence that perceived patterns evoked
507 by multi-electrode stimulation are maintained both within and across sessions. Similar results were found
508 for BS1, but in that case we could not make a within vs. across session comparison for absolute mapping
509 data (Figure 6A, C – E).

510

511 *Structure captured by multi-point sequence mapping*

512

513 Multi-point relative mapping with sampling of specific rows on the electrode array captured some key
514 expected features of functional organization of early visual cortex, based on work in sighted subjects
515 [4,33,34]. This is illustrated with a set of sequences sampled in subject BS2 (Figure 7). The two electrode
516 rows sampled that lie below the calcarine fissure on the brain (red and orange) produce phosphenes in the
517 upper visual field as expected, with posterior electrodes in both rows evoking more foveal percepts and
518 more anterior electrodes producing phosphenes in increasing eccentricity. The rows of electrodes just
519 superior to the calcarine (yellow-orange and light green) similarly produced phosphenes that lie along iso-
520 angle lines in visual space in the lower visual field, with more anterior electrodes producing more
521 eccentric phosphenes. Movement from the row closest to the calcarine fissure (yellow-orange) to the next
522 row further superior (light green) results in phosphenes found closer to the vertical meridian (VM) as is
523 expected for superior movement within area V1 above the calcarine fissure. As rows are examined that lie
524 further superior to the calcarine (dark green, light blue and dark blue), moving into area V2, the
525 progression of the phosphenes reversed in visual space, with progressive movement away from the VM.

526

527 Although structured sampling using rows on the electrode array provided some useful information, there
528 was additional complexity that was revealed when we examined the full set of sequences from each
529 subject (Figure S1). Spatial relationships for a given set of electrodes determined by sampling with one
530 sequence may conflict with those determined by sampling with other sequences, despite being internally

531 consistent within and across sessions. Furthermore, there was a tendency for subjects to regularize the
532 reported space between phosphenes obtained with multi-electrode stimulation. For example, when
533 presenting a sequence of electrodes that produce phosphenes at increasing eccentricities, such as
534 electrodes 56 – 60 in BS2, the subject tended to report equal spacing between each perceived phosphene,
535 rather than reporting more space between the more eccentric phosphenes. This pattern of regular spacing
536 was consistently observed across sequences at all eccentricities evaluated (BS1: 4.3 – 31°; BS2: 2.4 –
537 26°). The trend towards regularization of distance between phosphenes was found for sequences whether
538 they generated straight lines of phosphenes in visual space or produced curved trajectories.

539
540 To quantify the observation that subjects tended to report regularized distance between phosphenes,
541 cortical magnification factor (CMF) was calculated for neighboring electrodes from multi-electrode
542 sequences, on each trial. The CMF values observed were consistent across different eccentricities (Figure
543 8, data points) and different from those predicted by a standard mapping in sighted subjects (Figure 8,
544 solid lines). This regularization of reported phosphene spacing was additionally demonstrated by
545 presenting sequences with the same end points on a row of electrodes, but varying the intermediary
546 electrodes presented (Figure 9). For example, if stimulation was delivered sequentially to electrodes 56,
547 57, and 58 (sequences 1 and 2, Figure 9A–B) the distance between phosphenes evoked by electrodes 56
548 and 58 (3.6°) was larger than if stimulation was delivered sequentially to only electrodes 56 and 58
549 (sequence 4, Figure 9D) (1.8°). When individual electrodes along this row were dropped from the
550 sequence, the subject nevertheless reported a consistently spaced set of phosphenes (Figures 9E–F).

551

552 *Limited structure apparent in absolute maps*

553

554 Maps of visual space based on absolute mapping were constructed by averaging the location of
555 individually mapped phosphenes. For both BS1 (Figure 10B) and BS2 (Figure 10E), maps constructed in

556 this manner do not reflect the highly structured representation of visual space expected for early visual
557 cortex. The only clear feature evident in these maps was that electrodes above the calcarine generally
558 produced phosphenes below the horizon and vice versa.

559

560 *Fitting a logarithmic map of visual space*

561

562 As described above, structured sampling of the electrode array using multi-electrode sequences was
563 partially effective at revealing the structure of visual field maps in early visual cortex, but could not
564 account for all complexity. We hypothesized a better estimate of the overall map in each subject could be
565 obtained by fitting a model of the V1-V3 complex to the data from multi-electrode sequences (Figure S2).
566 The Banded Double-Sech model [39] fit to the data assumes a logarithmic mapping of each visual area,
567 and was adjusted for each subject by a scaling factor (BS1: 20.4; BS2: 24.5). The placement of the array
568 structure on the flat map of cortex was optimized by minimizing the average weighted displacement
569 between the cortical projection of phosphenes and the associated electrodes within the array structure
570 (BS1: $V1_{UF} = 2.8$ mm, $V1_{LF} = 1.4$ mm, $V2_{UF} = 2.9$ mm; BS2: $V1_{UF} = 0.40$ mm, $V1_{LF} = 1.9$ mm, $V2_{LF} =$
571 1.5 mm). The visual field maps based on the V1-V3 model fit to multipoint data (Figure 10C and F) had
572 clear internal structure reflective of the organization found with multi-point sequences, but additionally
573 provided logarithmic spacing between phosphenes that was not well captured by multi-point sequences.

574

575

576 **Discussion**

577

578 *Sighted vs blind subjects*

579

580 We evaluated the reliability of phosphene reporting in both sighted and blind subjects. We found absolute
581 mapping yields consistent, reliable results in sighted participants, but significantly more variability with
582 blind participants. Blind subjects had over 8 times the variability in reporting phosphene location
583 compared to their sighted counterparts. Possible reasons for this include differences in testing setup,
584 changes to functional organization of visual cortex in blind subjects, and differences in the ability of blind
585 subjects to compensate for shifts in body, head, or eye position.

586

587 There were notable differences in the exact framework used for phosphene mapping and in the set of
588 parameters used for electrical stimulation in the two groups tested. This was due to both the timeframe in
589 which each set of experiments occurred, and limitations of the stimulation system used to test in the blind
590 subjects. The small differences in electrical stimulation trains, however, were unlikely to impact these
591 experiments. Differences in stimulation frequency, pulse width, were likely to create changes in the exact
592 current required for perception of a phosphene and could potentially impact the size or brightness of the
593 perceived phosphenes. In all testing, current amplitudes were adjusted so that each subject could clearly
594 perceive and locate the phosphene. We have no reason to believe small changes in stimulation parameters
595 would have impacted the subjects' ability to precisely locate phosphenes. A much larger difference
596 between the two experiments was the way in which subjects fixated. Sighted subjects used visual fixation
597 whereas blind subjects used tactile fixation. This was a necessary change, and very likely to impact
598 performance.

599

600 The disparity in precision between blind and sighted subjects may partly be explained by blind
601 participants being more impacted by positional errors associated with absolute mapping. Positional errors
602 – which include small shifts between the subject and the reporting monitor, gaze angle, fixation strategy,
603 and pointing response – have been described as a central weakness of absolute mapping [40]. Sighted
604 subjects had minimal scatter between subsequent trials for a given phosphene, indicating whatever
605 positional errors they faced were easily overcome, likely compensated for with subtle shifts in body

606 position or gaze angle. Positional errors conversely seem to compound in blind subjects, resulting in shifts
607 of several degree across reported location for a single phosphene.

608

609 Blind subjects may be more susceptible to positional errors for several reasons. Blind participants cannot
610 use the same visual cues to align themselves in front of the monitor and fixation point or to compensate
611 for the subtle shifts in body and head position that occur during testing. There are also likely unaccounted
612 errors from eye position, which is an issue of considerable importance to both the process of mapping and
613 the continued development of cortical prostheses [41]. Blind individuals typically have more difficulty
614 maintaining a steady gaze angle or may have a nystagmus that causes unpredictable shifts in eye position
615 [42], [43], making consistent fixation a challenge and contributing to positional jitter. For these reasons,
616 regularizing the setup and introducing elements to help the subject self-center were imperative.

617

618 Positional errors also affect the reporting phase of the task. Reporting phosphene location by pointing to it
619 on a monitor relies heavily on proprioception. Visual feedback normally updates this internal
620 representation of body position and plays a central role in planning trajectory and kinematics of reaching
621 movements [44]. Without visual feedback, positional drift occurs [45]. Blind subjects lack this visual
622 feedback and cannot correct placement by visually aligning their pointing finger with the phosphene
623 location. With this in mind, we focused on implementing a fixation strategy that could provide an
624 alternative means to update proprioception by reinforcing the location of the fixation point with the
625 reporting hand.

626

627 *Improvements to fixation strategy or reference frame*

628

629 Previous literature, with sighted participants and simulated phosphenes, indicated that improving tactile
630 feedback increased the reliability and accuracy of phosphene localization [46]. By instructing the strategic
631 use of both hands and employing a tactile board on which the subjects were to respond reduced error by a

632 factor of two to three. Stronks and Dagnelie [40] employed a similar fixation strategy in their simulated
633 studies, having subjects place both index fingers side-by-side. Here we are able to build on this earlier
634 work by directly comparing two forms of tactile fixation in blind subjects with phosphenes evoked by
635 electrical stimulation of cortex.

636

637 Bimanual fixation improved precision by 2 to 3 times compared to unimanual fixation. This supports our
638 hypothesis that a providing additional proprioceptive feedback can indeed improve reporting precision for
639 blind subjects. In the context of mapping, making consistent physical connection between the hand used
640 for fixation and the hand used for reporting phosphene location provides a simple way to update
641 proprioception [44]. Further improvements to the framework for reporting phosphenes are possible and
642 should be the subject of future investigations. It may be advantageous, for example, to use tactile markers
643 to establish vertical and horizontal axes or to incorporate a tactile grid [40].

644

645 *Improvements to mapping strategy*

646

647 Although the bimanual tactile fixation strategy did improve the reliability of phosphene mapping in both
648 blind subjects tested, it did not increase precision to the level achieved by sighted subjects. Relative
649 mapping utilizing stimulation of multiple electrodes on each trial allows the assessment of the location of
650 one phosphene relative to another, rather than relating each individual phosphene to a central, body-
651 external, tactile fixation point. Without alignment across trials, subjects contend with the same difficulties
652 in localizing phosphenes experienced during absolute mapping, such as an inability to make subtle
653 corrections to their gaze angle or body positions. However, once variations in absolute placement are
654 removed, precision was significantly improved. The precision for a single phosphene mapped with this
655 relative approach in blind subjects was similar to the same range of values as sighted persons performing
656 absolute mapping.

657

658 *Trial-to-trial variability*

659

660 Most variability across trials was explained by three main components: translation, rotation, and scale.

661 These observed trial variants may have different origins and likely have different impacts on VCP

662 functionality that vary by task. Translation, or shifts in the absolute location of the pattern, was the largest

663 component of trial variability. This type of variability would mostly impact localization tasks in daily

664 activities, especially when holding a steady gaze or camera angle. Small changes in gaze direction or

665 body position at the start of each trial are likely to explain a large portion of the observed variation, and it

666 may be adequately addressed in future devices with integrated eye tracking. Perceived rotation of a

667 phosphene pattern was the next largest trial variation observed. Rotational deviations were typically

668 minimal but, on occasion, presented as a pattern nearly orthogonal to its typical orientation. In a low

669 context environment, this could mean certain simple shapes or characters could be easily confused. The

670 reason for pattern rotation is unclear, but we theorize it is related to subjects' ability to form a stable

671 framework for phosphene reporting and that improving the reporting framework during testing or adding

672 more visual context to a presented scene in free-viewing may reduce the likelihood of large rotational

673 variations. Changes in scale were the smallest contributor to imprecision, and presumably will have less

674 of an impact on operational use than translational or rotational deviations. Scaling variations may relate to

675 the distance or plane at which phosphenes are perceived. Importantly, when any of these variations

676 occurred, there was no internal distortion to the phosphene pattern. The whole form was rotated, shifted, or

677 scaled, and the internal structure of the pattern remained intact.

678

679 *Maintenance of pattern*

680

681 Despite trial-to-trial variability in the exact location, orientation, or scale, the internal spatial relationships

682 among phosphenes in a sequence were robustly maintained across multiple sessions. Previous

683 experiments have implied that spatial patterns of phosphenes were maintained and could be used to make

684 simple discriminations [21], [34], [47], but had not quantitatively examined this observation in detail.

685 Here we present strong evidence that simple spatial patterns are consistently perceived over time (Figure
686 6A-C), and that the perceived spatial configuration of phosphenes evoked by a sequence of electrodes is
687 similar whether presented as its own sequence or as part of a larger pattern (Figure 6D-F).

688

689 Robust maintenance of phosphene patterns is important for multiple reasons. First, it demonstrates that
690 structured mapping is likely retained in early visual cortex several years after late onset of blindness.

691 Second, it is the key feature that makes multi-electrode sequences useful in obtaining precise locations of
692 phosphenes associated with each electrode. Because spatial relationships are robustly maintained, relative
693 mapping is useful in parsing fine spatial details between phosphenes. Third, it has important implications
694 for the ability of future VCP users to perform specific daily tasks. Stable phosphene patterns suggests
695 VCP users will be able to reliably use patterned sequences of phosphenes to recognize simple shapes or
696 forms. In support of this premise, previous work showed dynamic stimulation of multi-electrode groups
697 could reliably convey several simple characters to blind subjects [21].

698

699 *Impact of mapping strategy on the measured structure of the map of visual space*

700

701 Maps of visual space determined by absolute mapping did not yield a structured representation of visual
702 space. The only clear feature captured by absolute mapping was the distribution of phosphenes evoked by
703 electrodes on either side of the calcarine fissure; electrodes above the calcarine generally, but not always,
704 produced phosphenes the subjects reported below the horizon and vice versa. The imprecision of the
705 method was not adequately offset by conducting many trials for each electrode. In this way, absolute
706 mapping was found to be both comparatively uninformative and inefficient at mapping visual space.

707

708 Relative mapping with multi-point sequences approached the task with structured sampling under an
709 assumption that visual cortex has a highly organized structure. This method was able to capture key

710 features similar to the known functional organization of early visual cortex as measured in sighted
711 subjects [14], [48], [17]. Beyond the general structure of phosphenes below the calcarine fissure
712 producing percepts in the upper visual field and vice versa, use of multi-point sequences yielded reports
713 of sets of phosphenes in visual space that lay in increasing eccentricities along iso-angle lines, and which
714 exhibited progression towards the VM with movement in the superior direction in area V1. Additionally,
715 sampling with rows of the electrode array located further superior to the calcarine, presumed in area V2,
716 then resulted in sets of phosphenes which progressed away from the VM as expected. However,
717 structured sampling along rows had other added complexity and some clear limitations.

718
719 Spatial relationships for a given set of electrodes determined by sampling with one sequence may conflict
720 with those determined in by sampling with other sequences, despite being internally consistent within and
721 across sessions. This may be related to the subjects' tendency to report regularized space between
722 phosphenes that were presented sequentially from stimulation on nearby electrodes. The reasons for these
723 observations are unclear but are unlikely to suggest the lack of a single robust map of early visual cortex.
724 While motor errors in the reporting phase of the tasks may contribute to the regularized intervals between
725 phosphenes, conversations with BS2 indicated he also perceived the phosphenes to occur at regularly
726 spaced intervals. We theorize the perceptual contribution to this effect may result from either blind
727 subjects implementing a different framework for performing visual tasks in low context environments, or
728 the small irregularities in the spatial shifts between phosphenes could be masked by the regular temporal
729 interval of their presentation. It will be important for future research to parse out the source of this
730 regularization to appropriately mitigate the effects.

731
732 We fit a model of the V1-V3 complex [39] to multi-point sequence data (Figure S1) to devise maps of
733 visual space that represented the structure found in these data while also incorporating expected changes
734 in CMF with eccentricity. Fitting a logarithmically spaced map to the scale and location of multi-point
735 sequences is similar to an atlas-based approach. Standard retinotopic atlases use average anatomical

736 landmarks or functional organization to fit the logarithmic structure of visual cortex to the conformal
737 topology of a subject's visual cortex, and have been shown to predict cortical retinotopy of out-group
738 sighted subjects with high accuracy [49]–[51]. An atlas approach may provide useful insights or a useful
739 basis for predicting phosphene location in blind subjects. However, the available atlases have not yet been
740 validated with blind subjects and unpredictable changes to visual cortex may occur after loss of sight
741 [22]–[26], that may result in a need to alter the scaling or landmarks used in a standard atlas to better
742 accommodate these variations. Because these atlases were developed on a sighted population and we are
743 naive to the ways plastic changes may have impacted visual cortex physiology after full vision loss, it is
744 important to validate the atlases on a blind population. For these reasons, our current implementation used
745 a model that assumes basic logarithmic mapping within each visual area but does not assume the location
746 or size of each visual area in relation to topological landmarks as is done when using standard atlases
747 based on fMRI data. Moving forward it would be advantageous to test phosphene maps extracted from
748 our hybrid approach and an atlas-based approach, as well as conduct a comprehensive validation of
749 retinotopic atlases on a blind subject group.

750

751 *Determining veridical structure of visual field maps in blind subject*

752

753 In addition to being reliable, phosphene maps should ideally be an accurate representation of the visual
754 space subtended by the electrode array. We are presently unable to claim which map is the most accurate
755 representation of each subject's visual space maps in early visual cortex. Earlier work in the field
756 functionally validated their phosphene maps by generating simple visual patterns from the map [34].
757 Similarly, we used the information derived from multi-point sequences to plan stimulation patterns in the
758 shape of letters [21]. In this experiment, stimulation was delivered sequentially to several electrodes to
759 dynamically trace a pattern through visual space. With no prior training, our subject, BS2, correctly
760 identified four different letter shapes (“W”, “N”, “M”, “U”) at 93% accuracy. Drawings produce by this
761 subject during this task show an alignment between the letter endpoints and the mapped phosphene

762 locations. This provides some confirmation that the multi-point method can provide accurate enough
763 information to plan and deliver simple, useful visual patterns to blind users of a VCP. Moving forward,
764 validity of different maps can be evaluated by planning simple character or shape sequences based on
765 differently generated maps and compare the perceptual experience reported by the subject.

766

767

768 **Conclusions**

769

770 Having a reliable and efficient way to obtain phosphene maps in individual blind subjects will likely be
771 important for the successful implementation of a new generation of VCPs. Our results demonstrate that
772 obtaining accurate phosphene maps in blind subjects is fraught with challenges, and results may heavily
773 depend on the exact techniques that are employed. Using the described methods to reinforce
774 proprioceptive feedback and focusing on mapping techniques that prioritize relative spatial relationships
775 can improve the confidence that the phosphene mapping data collected is reflective of the underlying
776 spatial maps in the visual cortex. Finally, standardized maps still provide utility and can be fit to
777 experimental data to provide a highly structured map, reflective of functional organization while retaining
778 nuanced details associated with each subject that may otherwise be lost. Ultimately, we recommend a
779 hybrid approach, fitting structured maps to the experimentally obtained location and scale of underlying
780 cortex.

781

782 **Acknowledgements**

783

784 The authors recognize the immense effort and time invested by the participants involved in this research
785 and acknowledge the assistance of Second Sight Medical Products. Funding for this research was
786 provided by NIH R01EY023336, and UH3NS103442.

787

788 **Conflict of interest**

789

790 We wish to draw the attention of the Editor to the following facts which may be considered as potential
791 conflicts of interest and to significant financial contributions to this work. At the time of data collection,
792 authors Michelle Armenta Salas, Uday Patel, Robert Greenburg, Jessy Dorn, and Nader Pouratian either
793 worked for or consulted for Second Sight Medical Products, the clinical trial sponsor and manufacturer of
794 the Orion Cortical Visual Prosthesis implanted in the blind subjects in this study.

795

796

797 [1] Second Sight Medical Products, “Early feasibility study of the Orion visual cortical prosthesis
798 system,” *clinicaltrials.gov*, Clinical trial registration NCT03344848, Aug. 2019. Available:
799 <https://clinicaltrials.gov/ct2/show/NCT03344848>

800 [2] Illinois Institute of Technology, “ICVP - A Phase I Clinical Trial to Determine the Feasibility of a
801 Human Cortical Visual Prosthesis for People with Blindness,” *clinicaltrials.gov*, Clinical trial
802 registration NCT04634383, Nov. 2020. Available: <https://clinicaltrials.gov/ct2/show/NCT04634383>

803 [3] E. Fernandez, “Pilot Study for the Development of a Cortical Visual Neuroprosthesis for the Blind
804 Based on Intracortical Microelectrodes,” *clinicaltrials.gov*, Clinical trial registration NCT02983370,
805 May 2020. <https://clinicaltrials.gov/ct2/show/NCT02983370>

806 [4] P. M. Lewis, H. M. Ackland, A. J. Lowery, and J. V. Rosenfeld, “Restoration of vision in blind
807 individuals using bionic devices: a review with a focus on cortical visual prostheses,” *Brain Res.*, vol.
808 1595, pp. 51–73, Jan. 2015, doi: 10.1016/j.brainres.2014.11.020.

809 [5] W. H. Bosking, M. S. Beauchamp, and D. Yoshor, “Electrical stimulation of visual cortex: relevance
810 for the development of visual cortical prosthetics,” *Annu. Rev. Vis. Sci.*, vol. 3, pp. 141–166, Sep.
811 2017, doi: 10.1146/annurev-vision-111815-114525.

- 812 [6] B. P. Christie, K. R. Ashmont, P. A. House, and B. Greger, "Approaches to a cortical vision
813 prosthesis: implications of electrode size and placement," *J. Neural Eng.*, vol. 13, no. 2, p. 025003,
814 Apr. 2016, doi: 10.1088/1741-2560/13/2/025003.
- 815 [7] R. M. Mirochnik and J. S. Pezaris, "Contemporary approaches to visual prostheses," *Mil. Med. Res.*,
816 vol. 6, Jun. 2019, doi: 10.1186/s40779-019-0206-9.
- 817 [8] W. Penfield and T. Rasmussen, *The cerebral cortex of man; a clinical study of localization of*
818 *function*. Oxford, England: Macmillan, 1950, pp. xv, 248.
- 819 [9] G. S. Brindley and W. S. Lewin, "The sensations produced by electrical stimulation of the visual
820 cortex," *J. Physiol.*, vol. 196, no. 2, pp. 479–493, 1968, doi:
821 <https://doi.org/10.1113/jphysiol.1968.sp008519>.
- 822 [10] M. Bak, J. P. Girvin, F. T. Hambrecht, C. V. Kufta, G. E. Loeb, and E. M. Schmidt, "Visual
823 sensations produced by intracortical microstimulation of the human occipital cortex," *Med. Biol. Eng.*
824 *Comput.*, vol. 28, no. 3, pp. 257–259, May 1990, doi: 10.1007/BF02442682.
- 825 [11] W. H. Dobbie and M. G. Mladejovsky, "Phosphenes produced by electrical stimulation of human
826 occipital cortex, and their application to the development of a prosthesis for the blind," *J. Physiol.*,
827 vol. 243, no. 2, pp. 553–576.1, Dec. 1974.
- 828 [12] G. S. Brindley, "Effects of electrical stimulation of the visual cortex," *Hum. Neurobiol.*, vol. 1, no. 4,
829 pp. 281–283, 1982.
- 830 [13] G. Holmes, "Disturbances of vision by cerebral lesions," *Br. J. Ophthalmol.*, vol. 2, no. 7, pp. 353–
831 384, Jul. 1918.
- 832 [14] R. B. Tootell, M. S. Silverman, E. Switkes, and R. D. Valois, "Deoxyglucose analysis of retinotopic
833 organization in primate striate cortex," *Science*, vol. 218, no. 4575, pp. 902–904, Nov. 1982, doi:
834 10.1126/science.7134981.
- 835 [15] J. C. Horton and W. F. Hoyt, "The representation of the visual field in human striate cortex. A
836 revision of the classic Holmes map," *Arch. Ophthalmol. Chic. Ill 1960*, vol. 109, no. 6, pp. 816–824,
837 Jun. 1991, doi: 10.1001/archophth.1991.01080060080030.

- 838 [16]S. A. Engel, G. H. Glover, and B. A. Wandell, "Retinotopic organization in human visual cortex and
839 the spatial precision of functional MRI," *Cereb. Cortex*, vol. 7, no. 2, pp. 181–192, Mar. 1997, doi:
840 10.1093/cercor/7.2.181.
- 841 [17]R. F. Dougherty, V. M. Koch, A. A. Brewer, B. Fischer, J. Modersitzki, and B. A. Wandell, "Visual
842 field representations and locations of visual areas V1/2/3 in human visual cortex," *J. Vis.*, vol. 3, no.
843 10, pp. 586–598, 2003, doi: 10.1167/3.10.1.
- 844 [18]B. A. Wandell and J. Winawer, "Imaging retinotopic maps in the human brain," *Vision Res.*, vol. 51,
845 no. 7, pp. 718–737, Apr. 2011, doi: 10.1016/j.visres.2010.08.004.
- 846 [19]W. H. Dobelle, J. Turkel, D. C. Henderson, and J. R. Evans, "Mapping the representation of the
847 visual field by electrical stimulation of human visual cortex," *Am. J. Ophthalmol.*, vol. 88, no. 4, pp.
848 727–735, Oct. 1979, doi: 10.1016/0002-9394(79)90673-1.
- 849 [20]S. Niketeghad *et al.*, "Phosphene perceptions and safety of chronic visual cortex stimulation in a
850 blind subject," *J. Neurosurg.*, vol. 132, no. 6, pp. 2000–2007, May 2019, doi:
851 10.3171/2019.3.JNS182774.
- 852 [21]M. S. Beauchamp *et al.*, "Dynamic stimulation of visual cortex produces form vision in sighted and
853 blind humans," *Cell*, vol. 181, no. 4, pp. 774–783.e5, May 2020, doi: 10.1016/j.cell.2020.04.033.
- 854 [22]E. Castaldi, C. Lunghi, and M. C. Morrone, "Neuroplasticity in adult human visual cortex," *Neurosci.*
855 *Biobehav. Rev.*, vol. 112, pp. 542–552, May 2020, doi: 10.1016/j.neubiorev.2020.02.028.
- 856 [23]J. Gothe, S. A. Brandt, K. Irlbacher, S. Rörich, B. A. Sabel, and B. Meyer, "Changes in visual cortex
857 excitability in blind subjects as demonstrated by transcranial magnetic stimulation," *Brain*, vol. 125,
858 no. 3, pp. 479–490, Mar. 2002.
- 859 [24]P. R. Silva *et al.*, "Neuroplasticity in visual impairments," *Neurol. Int.*, vol. 10, no. 4, Art. no. 4, Dec.
860 2018, doi: 10.4081/ni.2018.7326.
- 861 [25]A. K. Andelin *et al.*, "The effect of onset age of visual deprivation on visual cortex surface area
862 across-species," *Cereb. Cortex*, vol. 29, no. 10, pp. 4321–4333, Sep. 2019, doi:
863 10.1093/cercor/bhy315.

- 864 [26]H. J. Park *et al.*, “Morphological alterations in the congenital blind based on the analysis of cortical
865 thickness and surface area,” *NeuroImage*, vol. 47, no. 1, pp. 98–106, Aug. 2009, doi:
866 10.1016/j.neuroimage.2009.03.076.
- 867 [27]E. Fernández *et al.*, “Development of a cortical visual neuroprosthesis for the blind: the relevance of
868 neuroplasticity,” *J. Neural Eng.*, vol. 2, no. 4, p. R1, Nov. 2005, doi: 10.1088/1741-2560/2/4/R01.
- 869 [28]B. S. Everitt and D. N. Rushton, “A method for plotting the optimum positions of an array of cortical
870 electrical phosphenes,” *Biometrics*, vol. 34, no. 3, pp. 399–410, Sep. 1978.
- 871 [29]W. H. Dobelle, “Artificial vision for the blind by connecting a television camera to the visual cortex,”
872 *ASAIJ*, vol. 46, no. 1, pp. 3–9, Feb. 2000.
- 873 [30]J. Winawer and J. Parvizi, “Linking electrical stimulation of human primary visual cortex, size of
874 affected cortical area, neuronal responses, and subjective experience,” *Neuron*, vol. 92, no. 6, pp.
875 1213–1219, Dec. 2016, doi: 10.1016/j.neuron.2016.11.008.
- 876 [31]W. H. Bosking *et al.*, “Saturation in phosphene size with increasing current levels delivered to human
877 visual cortex,” *J. Neurosci.*, vol. 37, no. 30, pp. 7188–7197, Jul. 2017, doi:
878 10.1523/JNEUROSCI.2896-16.2017.
- 879 [32]W. H. Dobelle, M. G. Mladejovsky, and J. P. Girvin, “Artificial vision for the blind: electrical
880 stimulation of visual cortex offers hope for a functional prosthesis,” *Science*, vol. 183, no. 4123, pp.
881 440–444, Feb. 1974, doi: 10.1126/science.183.4123.440.
- 882 [33]G. S. Brindley, “Sensory effects of electrical stimulation of the visual and paraviscual cortex in man,”
883 in *Visual Centers in the Brain*, G. Berlucchi, G. S. Brindley, B. Brooks, O. D. Creutzfeldt, E. Dodt,
884 R. W. Doty, H.-J. Freund, C. G. Gross, D. A. Jeffreys, R. Jung, U. Kuhnt, D. M. MacKay, E. Marg,
885 N. Negrão, G. Rizzolatti, J. M. Sprague, G. Székely, J. Szentágothai, D. Whitteridge, and R. Jung,
886 Eds. Berlin, Heidelberg: Springer, 1973, pp. 583–594. doi: 10.1007/978-3-642-65495-4_14.
- 887 [34]W. H. Dobelle, M. G. Mladejovsky, J. R. Evans, T. S. Roberts, and J. P. Girvin, “‘Braille’ reading by
888 a blind volunteer by visual cortex stimulation,” *Nature*, vol. 259, no. 5539, Art. no. 5539, Jan. 1976,
889 doi: 10.1038/259111a0.

- 890 [35]B. Fischl, M. I. Sereno, and A. M. Dale, "Cortical surface-based analysis. II: Inflation, flattening, and
891 a surface-based coordinate system," *NeuroImage*, vol. 9, no. 2, pp. 195–207, Feb. 1999, doi:
892 10.1006/nimg.1998.0396.
- 893 [36]A. M. Dale, B. Fischl, and M. I. Sereno, "Cortical surface-based analysis. I. Segmentation and
894 surface reconstruction," *NeuroImage*, vol. 9, no. 2, pp. 179–194, Feb. 1999, doi:
895 10.1006/nimg.1998.0395.
- 896 [37]R. W. Cox, "AFNI: software for analysis and visualization of functional magnetic resonance
897 neuroimages," *Comput. Biomed. Res. Int. J.*, vol. 29, no. 3, pp. 162–173, Jun. 1996, doi:
898 10.1006/cbmr.1996.0014.
- 899 [38]Z. S. Saad, R. C. Reynolds, B. Argall, S. Japee, and R. W. Cox, "SUMA: An interface for surface-
900 based intra- and inter-subject analysis with AFNI," in *2004 2nd IEEE International Symposium on*
901 *Biomedical Imaging: Macro to Nano (IEEE Cat No. 04EX821)*, Arlington, VA, USA, 2004, vol. 2,
902 pp. 1510–1513. doi: 10.1109/ISBI.2004.1398837.
- 903 [39]M. M. Schira, C. W. Tyler, B. Spehar, and M. Breakspear, "Modeling magnification and anisotropy
904 in the primate foveal confluence," *PLOS Comput. Biol.*, vol. 6, no. 1, p. e1000651, Jan. 2010, doi:
905 10.1371/journal.pcbi.1000651.
- 906 [40]H. C. Stronks and G. Dagnelie, "Phosphene mapping techniques for visual prostheses," in *Visual*
907 *Prosthetics: Physiology, Bioengineering, Rehabilitation*, G. Dagnelie, Ed. Boston, MA: Springer US,
908 2011, pp. 367–383. doi: 10.1007/978-1-4419-0754-7_19.
- 909 [41]N. Paraskevoudi and J. S. Pezaris, "Eye movement compensation and spatial updating in visual
910 prosthetics: mechanisms, limitations and future directions," *Front. Syst. Neurosci.*, vol. 12, 2019, doi:
911 10.3389/fnsys.2018.00073.
- 912 [42]R. J. Leigh and D. S. Zee, "Eye movements of the blind.," *Invest. Ophthalmol. Vis. Sci.*, vol. 19, no.
913 3, pp. 328–331, Mar. 1980.
- 914 [43]K. R. Sherman and E. L. Keller, "Vestibulo-ocular reflexes of adventitiously and congenitally blind
915 adults," *Invest. Ophthalmol. Vis. Sci.*, vol. 27, no. 7, pp. 1154–1159, Jul. 1986.

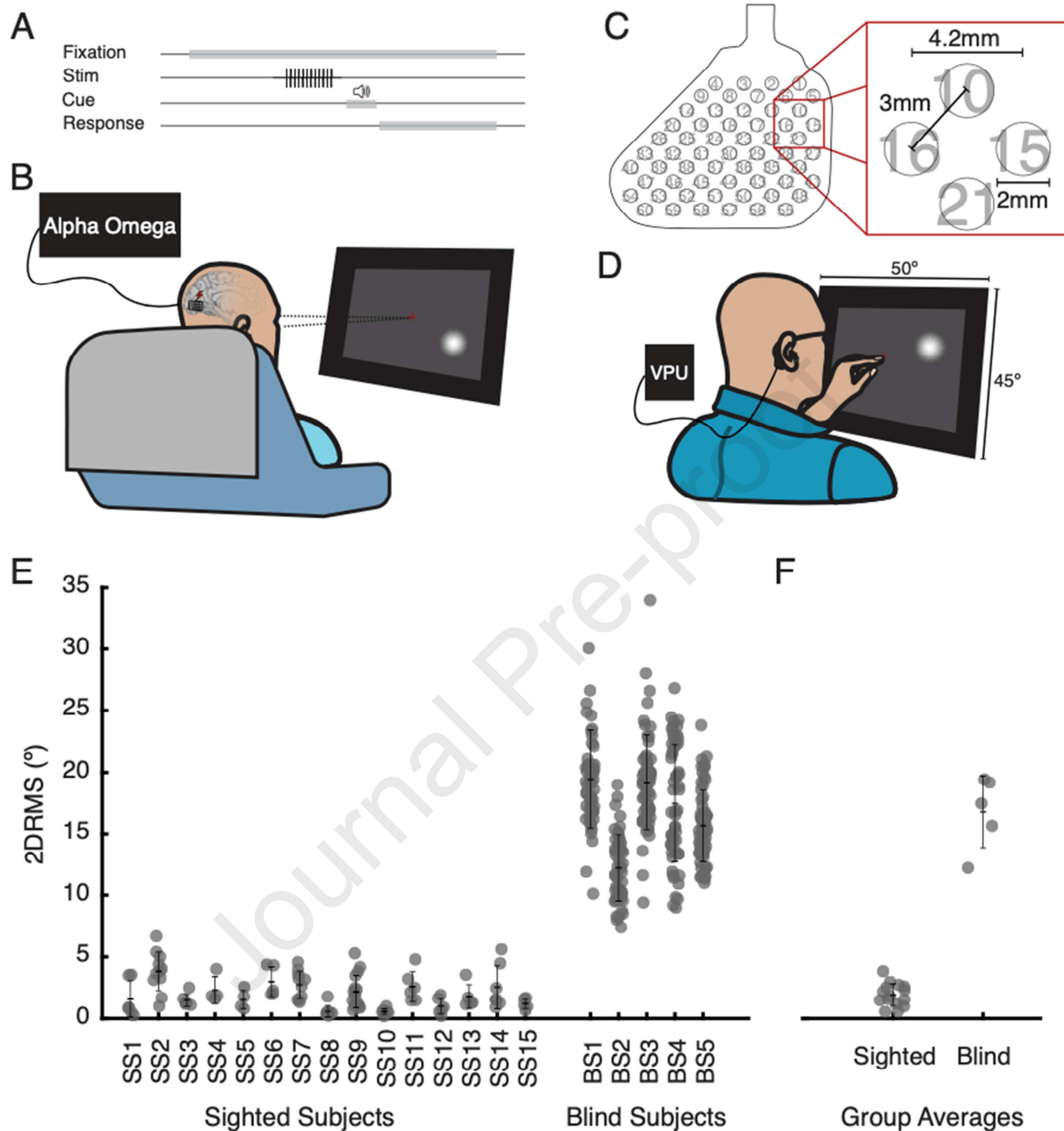
- 916 [44]F. R. Sarlegna and R. L. Sainburg, “The roles of vision and proprioception in the planning of
917 reaching movements,” *Adv. Exp. Med. Biol.*, vol. 629, pp. 317–335, 2009, doi: 10.1007/978-0-387-
918 77064-2_16.
- 919 [45]L. E. Brown, D. A. Rosenbaum, and R. L. Sainburg, “Movement speed effects on limb position
920 drift,” *Exp. Brain Res.*, vol. 153, no. 2, pp. 266–274, Nov. 2003, doi: 10.1007/s00221-003-1601-7.
- 921 [46]L. Zhang, X. Chai, S. Ling, J. Fan, K. Yang, and Q. Ren, “Dispersion and accuracy of simulated
922 phosphene positioning using tactile board,” *Artif. Organs*, vol. 33, no. 12, pp. 1109–1116, Dec. 2009,
923 doi: 10.1111/j.1525-1594.2009.00826.x.
- 924 [47]X. Chen, F. Wang, E. Fernandez, and P. R. Roelfsema, “Shape perception via a high-channel-count
925 neuroprosthesis in monkey visual cortex,” *Science*, vol. 370, no. 6521, pp. 1191–1196, Dec. 2020,
926 doi: 10.1126/science.abd7435.
- 927 [48]E. A. DeYoe *et al.*, “Mapping striate and extra striate visual areas in human cerebral cortex,” *Proc.*
928 *Natl. Acad. Sci.*, vol. 93, no. 6, pp. 2382–2386, Mar. 1996, doi: 10.1073/pnas.93.6.2382.
- 929 [49]L. Wang, R. E. B. Mruczek, M. J. Arcaro, and S. Kastner, “Probabilistic maps of visual topography
930 in human cortex,” *Cereb. Cortex*, vol. 25, no. 10, pp. 3911–3931, Oct. 2015, doi:
931 10.1093/cercor/bhu277.
- 932 [50]N. C. Benson, O. H. Butt, R. Datta, P. D. Radoeva, D. H. Brainard, and G. K. Aguirre, “The
933 retinotopic organization of striate cortex is well predicted by surface topology,” *Curr. Biol.*, vol. 22,
934 no. 21, pp. 2081–2085, Nov. 2012, doi: 10.1016/j.cub.2012.09.014.
- 935 [51]N. C. Benson, O. H. Butt, D. H. Brainard, and G. K. Aguirre, “Correction of distortion in flattened
936 representations of the cortical surface allows prediction of V1-V3 functional organization from
937 anatomy,” *PLoS Comput. Biol.*, vol. 10, no. 3, Mar. 2014, doi: 10.1371/journal.pcbi.1003538.

938

939

940

941



942

943 Figure 1. Discrepancy in reported phosphene precision between sighted and blind subjects. A. Task flow.

944 Subjects were instructed to fixate on a point on a touchscreen monitor placed in front of them at eye level,

945 while a pulse train of electrical stimulation was delivered to a single electrode. An auditory tone indicated

946 the end of stimulation and cued subjects to report the phosphene location. B. Sighted subjects conducted

947 tasks seated in their hospital bed and directed their gaze toward a centrally located fixation cross.

948 Stimulation was delivered by an Alpha Omega neural stimulator. Subjects reported location of

949 phosphenes on touchscreen display. C. Electrode array implanted in blind subjects. Contact numbers are
950 indicated from 1 (upper right) to 60 (lower left). D. Blind subjects were seated in a chair in a laboratory
951 testing room and fixated by placing their left index finger on a tactile point on the monitor. Electrical
952 stimulation was delivered by the Visual Processing Unit (VPU) of their Orion VCP. Subjects indicated
953 the location of the perceived phosphene with their right index finger. E. Precision in reported phosphene
954 location, quantified as 2DRMS, for individual sighted (SS1 – SS15) and blind subjects (BS1 – BS5). Each
955 data point reflects 2DRMS for an individual electrode. Error bars indicate mean and one standard
956 deviation. F. Group precision (sighted *vs.* blind) data. Each point reflects the average precision (2DRMS)
957 for a subject, across all electrodes evaluated for that subject. Error bars indicate group average and
958 standard deviation.

959

960

961

962

963

964

965

966

967

968

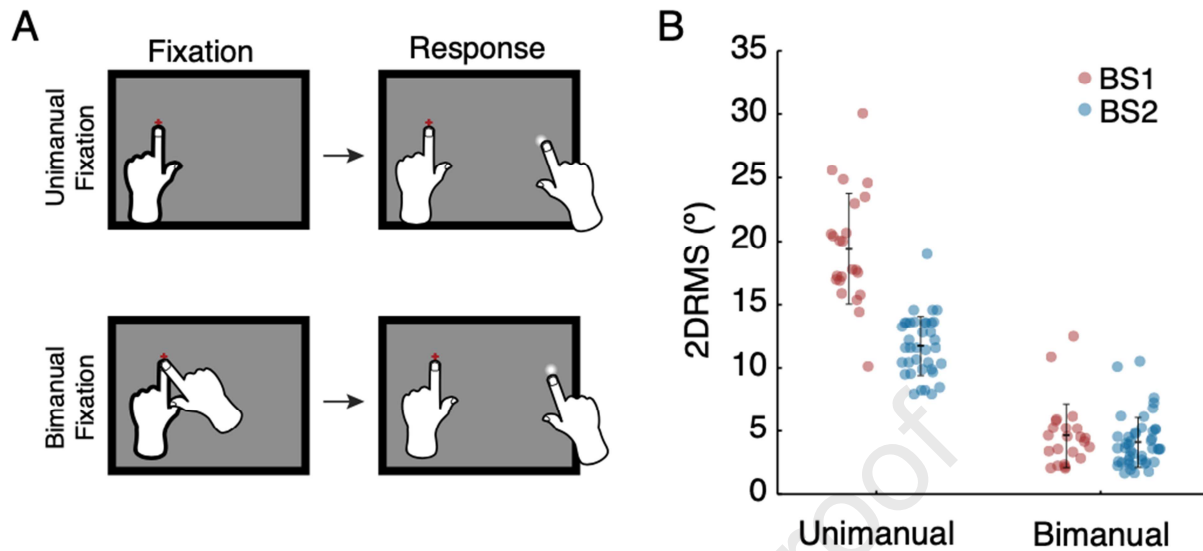
969

970

971

972

973



974

975 Figure 2. Precision of reported phosphene location for unimanual and bimanual fixation. A. Task

976 descriptions. Unimanual fixation (top), for which subjects fixated with their left index finger and report

977 with their right index finger. For bimanual fixation (bottom), subjects placed both left and right index

978 fingers on the fixation point, then reported phosphene location with their right index finger, while leaving

979 their left index finger on the tactile fixation point. B. Precision for bimanual and unimanual fixation for

980 BS1 (red) and BS2 (blue). Each data point reflects precision (2DRMS) for a single electrode. Error bars

981 indicate mean and standard deviation.

982

983

984

985

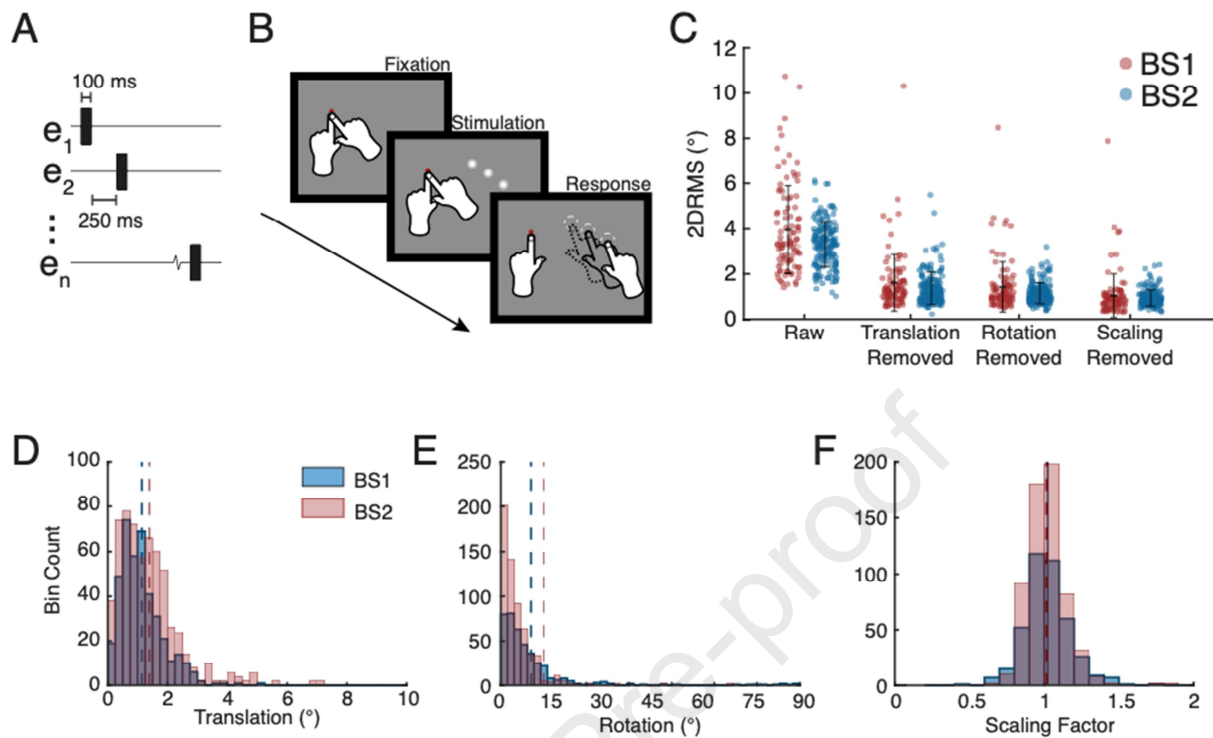
986

987

988

989

990



991

992 Figure 3. Improvement in precision of phosphene reporting with relative mapping and types of variations

993 present in individual trials. A. Stimulation sequence timing used for multi-point relative mapping for BS2.

994 B. Illustration of multi-point relative mapping task. Multiple electrodes were stimulated on each trial and

995 then the subjects reported the location of each phosphene perceived, in the order experienced. C.

996 Precision of phosphene reporting with relative mapping with multi-point sequences. Each point represents

997 precision (2DRMS) for phosphenes evoked by stimulation of a single electrode, black error bars indicate

998 mean \pm standard deviation. The first column, labeled “Raw”, indicates data with no trial-to-trial

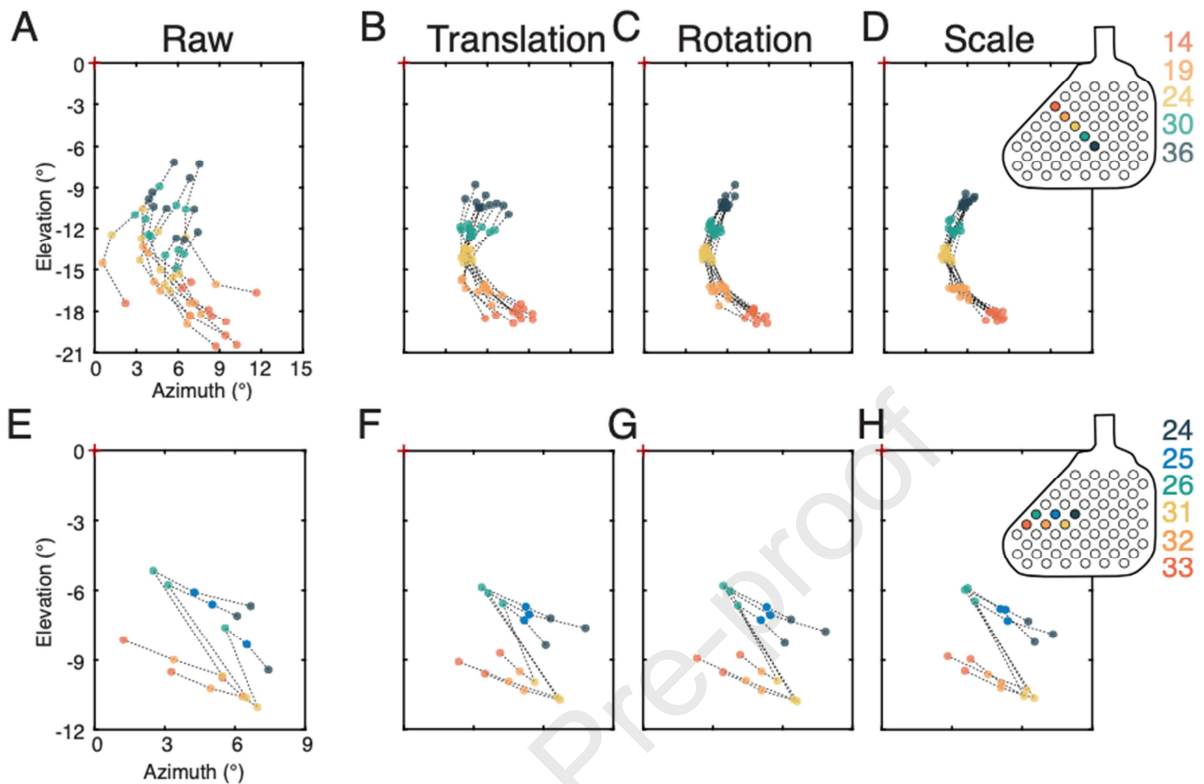
999 alignment. Subsequent columns reflect precision following removal of translational, rotational, and

1000 scaling variations. D. Frequency histogram indicating distribution of magnitude of translational variation

1001 for each subject for each trial. Averages for each parameter are indicated with a dashed line. E. Frequency

1002 histogram of rotational variation for each trial. F. Frequency histogram of scaling variation.

1003



1004

1005

1006

1007

1008

1009

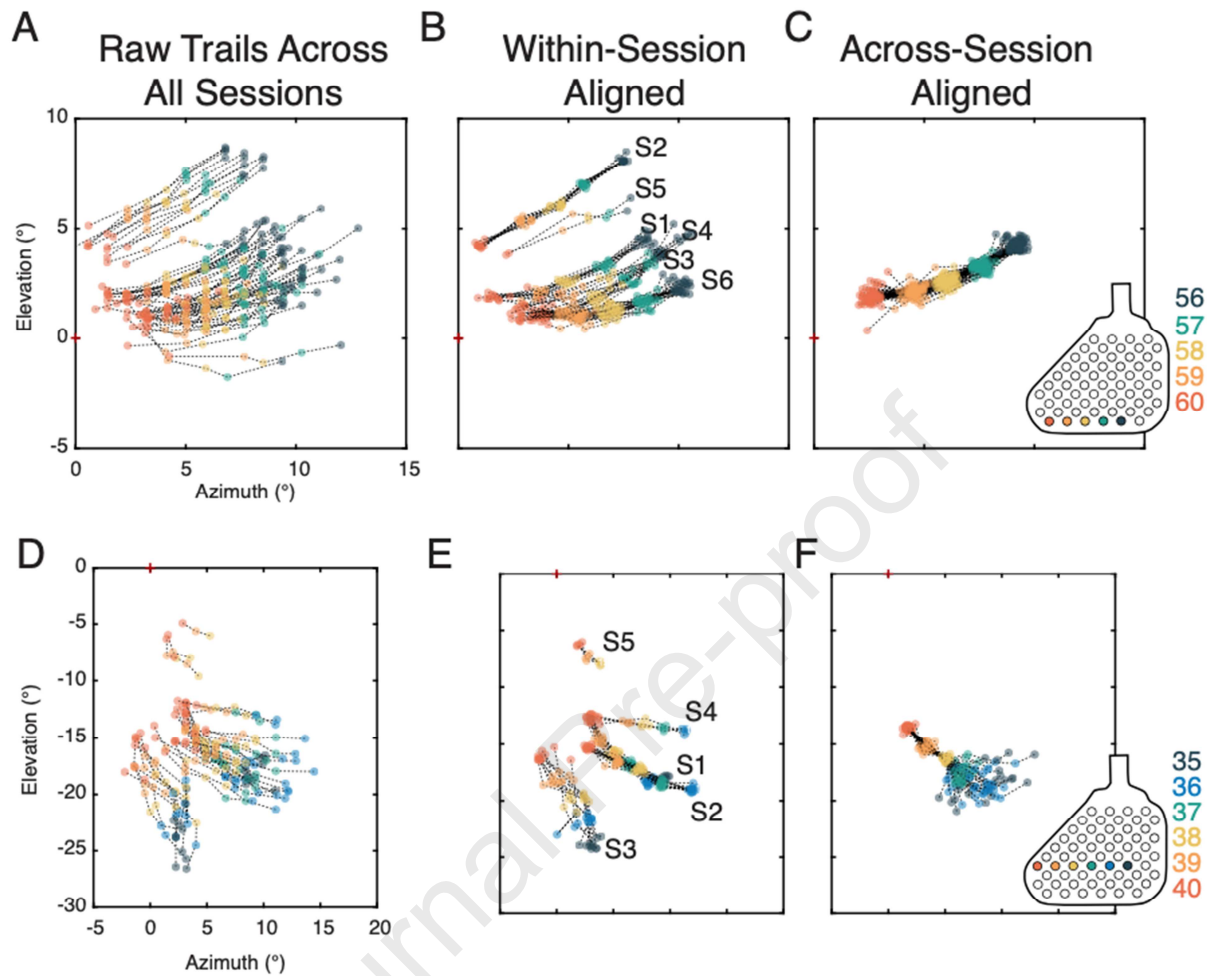
1010

1011

1012

1013

Figure 4. Maintenance of spatial configuration of phosphenes within sessions. A. A five-electrode sequence presented to BS2. Location and orientation of raw trials. B. Same trials after removal of translational deviations by aligning trials to the center of mass across all trials. C. Same set of trials following removal of rotational variation. D. Same set of trials after removal of scaling variation. The internal structure of the pattern is robustly maintained and clearly visible once shifts and rotations in space are removed. Array inset indicates electrodes used in this sequence. E-H. A second example from the same subject illustrating results with a multi-electrode pattern in the shape of a simple character. E. Raw trials are shown in this panel. F. Trials with translational variations removed. G. Trials with rotational variation removed. H. Trials with scaling variation removed.



1014

1015 Figure 5. Maintenance of spatial configuration of phosphenes across multiple sessions. A – C. Stimulation

1016 delivered to electrode sequence 56-57-58-59-60 presented during each of the 6 different sessions. A. All

1017 raw trials of this sequence collected across all sessions. B. Trials aligned by the session in which they

1018 were collected. C. All trials aligned across all sessions. Inset indicates the location of the electrodes on the

1019 array. D – F. Electrode sequences encompassing electrodes 35-36-37-38-39-40 with a subset of the

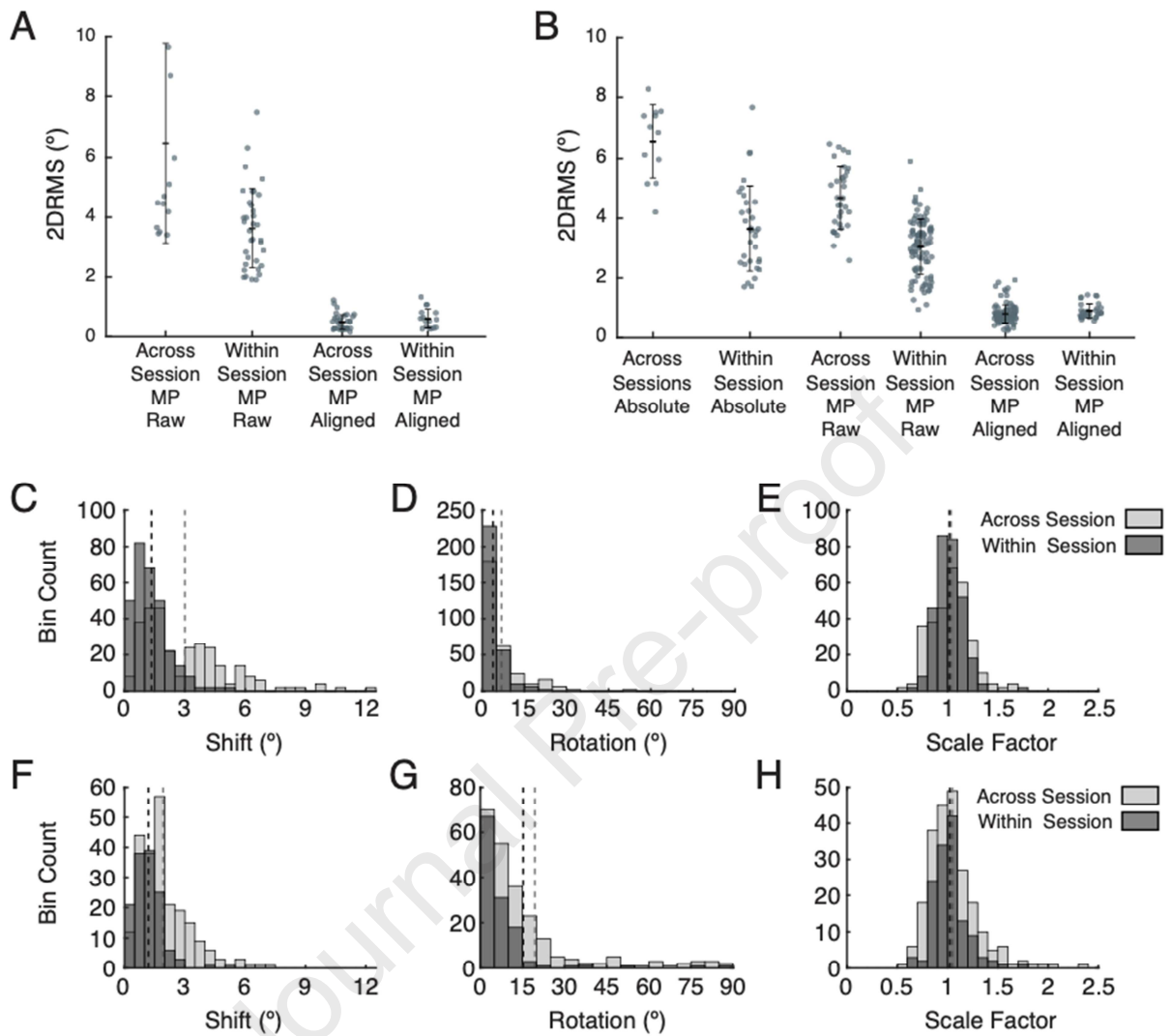
1020 electrodes (38-39-40) repeated during five separate sessions. D. All raw trials across all sessions. E. Trials

1021 aligned by the session in which they were collected. F. Trials aligned across all sessions using the

1022 electrodes that were common to all sequences (38-39-40).

1023

1024



1025

1026

1027

1028

1029

1030

1031

1032

1033

1034

Figure 6. Precision of phosphene mapping within and across sessions and dependence on trial-to-trial

variation in translation, rotation, and scaling. A. Precision within and across sessions for multi-point

mapping for BS1. Left two segments show precision prior to any alignment (across vs. within session,

$6.5 \pm 3.3^\circ$ vs. $3.6 \pm 1.3^\circ$). The right two segments indicate precision after removal of trial-to-trial

translational, rotational, and scaling variations (across vs. within session, $0.49 \pm 0.27^\circ$ vs. $0.61 \pm 0.34^\circ$). B.

Precision within and across session for absolute and multi-point mapping for BS2. The two segments on

the left indicate precision for reported phosphene locations determine through absolute mapping (across

vs. within session, $6.5 \pm 1.2^\circ$ vs. $3.6 \pm 1.4^\circ$). The middle two segments show precision for reported

phosphene locations determined with multi-point relative mapping (across vs. within session, $4.7 \pm 1.1^\circ$ vs.

1035 $3.0\pm 0.94^\circ$). The last two segments indicate precision for multi-point mapped phosphenes after removal of
1036 translational, rotational, and scaling variation (across *vs.* within session, $0.80\pm 0.32^\circ$ *vs.* $0.91\pm 0.25^\circ$). C –
1037 E. Frequency histograms showing the magnitude of each type of alignment deviation for multi-point
1038 sequences across (light gray) and within (dark gray) sessions for BS1. Dashed lines indicate means for
1039 each distribution. C. Translational variation (across *vs.* within session, *mean* 3.0° *vs.* 1.3°). D. Rotational
1040 variation (across *vs.* within session, *mean* 6.9° *vs.* 3.4°). E. Scale variation (across *vs.* within session, *std*
1041 0.19 *vs.* 0.14). F – H. Frequency histograms showing the magnitude of each type of alignment variation
1042 across and within sessions for BS2. F. Translation variation (across *vs.* within session, *mean* 1.9° *vs.*
1043 1.2°). G. Rotation variation (across *vs.* within session, *mean* 19° *vs.* 15°). H. Scale variations for BS2
1044 (across *vs.* within session, *std* 0.19 *vs.* 0.16).

1045

1046

1047

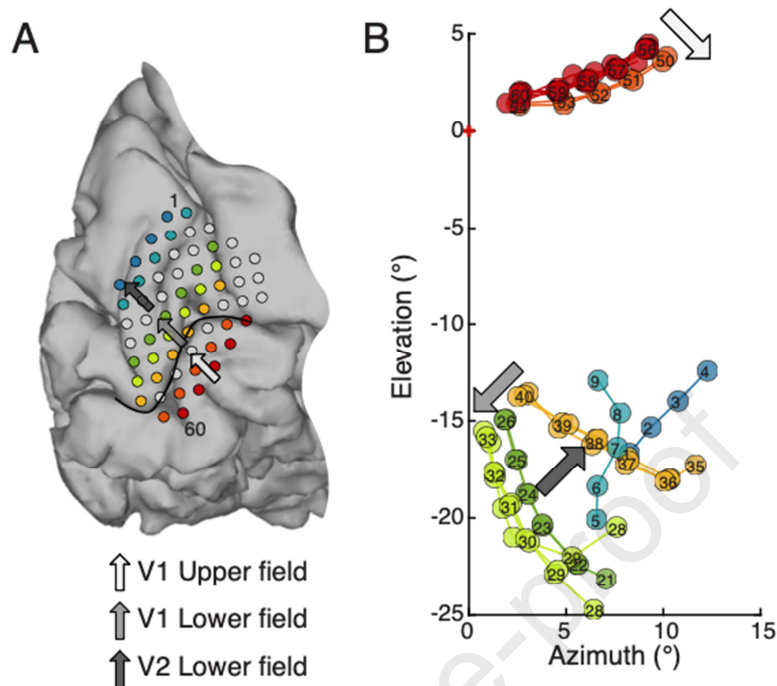
1048

1049

1050

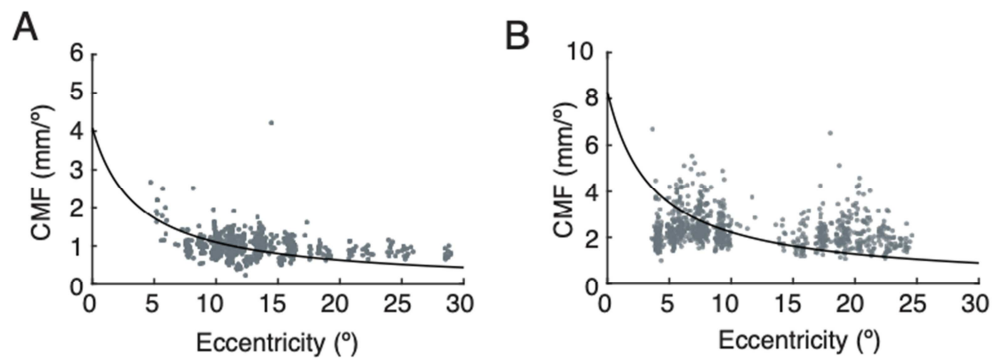
1051

1052



1053

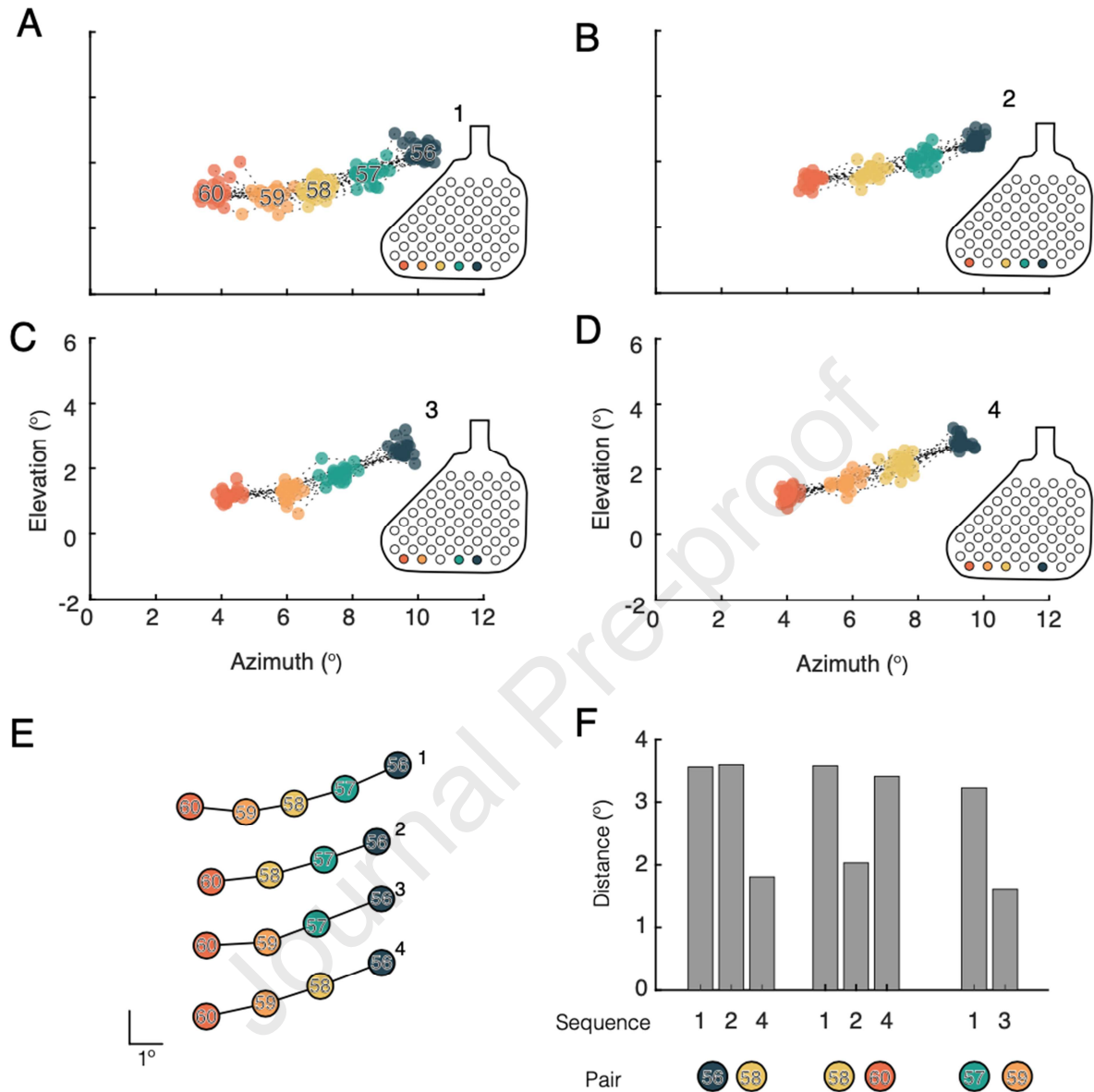
1054 Figure 7. Relative mapping with multi-point sequences captures key attributes of functional organization
 1055 of early visual cortex. A. BS2 electrode overlay on brain. A set of multi-point sequences were selected
 1056 that correspond to rows on the electrode array (colored rows). Arrows show progress across different
 1057 visual field representations. The light gray arrow points towards the calcarine, in an area representing
 1058 upper visual field of V1. The median gray arrow points towards the superior rows of the array, away from
 1059 the calcarine in an area of cortex representing lower visual field of V1. The dark gray arrow continues the
 1060 trajectory away from the calcarine fissure and towards the top row of the array. It approximately indicates
 1061 progression into the lower visual field representation of V2. B. Location of phosphenes obtained with
 1062 stimulation of each of the rows indicated in A in the same color. The arrows on the visual field map
 1063 indicate the progression in the visual field for phosphenes evoked by the corresponding electrode
 1064 sequences in the V1 upper field representation (light gray), V1 lower field (median gray), and V2 lower
 1065 field (dark gray).



1066

1067 Figure 8. Cortical magnification factor measured for phosphenes evoked by neighboring electrodes within
1068 multi-point sequence. Analysis was restricted to electrodes in V1. A. CMF across all multi-point sequence
1069 trials for BS1. Each point is CMF calculated for a pair of phosphenes on a single trial. Black lines indicate
1070 expected pattern of CMF across eccentricity based on the visual mapping function described in methods.

1071 B. CMF across all multi-point sequence trials for BS2.



1072

1073 Figure 9. Examples indicating regularization of reported phosphene locations when using multi-point

1074 sequences. A. Phosphene locations evoked on all trials of sequence 1(56, 57, 58, 59, and 60). B – D.

1075 Three patterns using the same row of electrodes tested in A, but with different electrodes dropped from

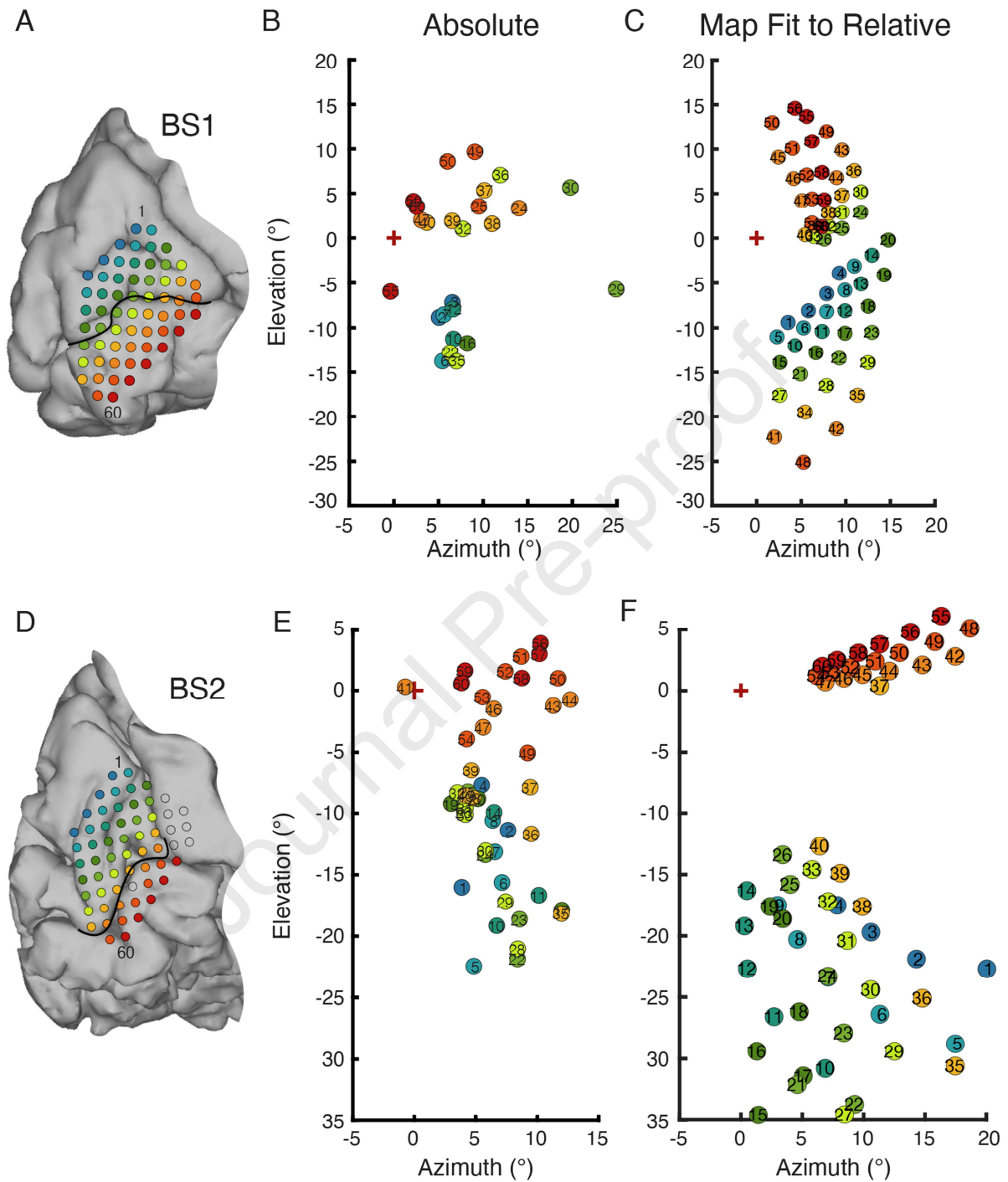
1076 the sequence. B. Phosphene locations evoked on all trials of sequence 2 (56, 57, 58, and 60). C.

1077 Phosphenes evoked by all trials of sequence 3 (56, 57, 59, and 60). D. Phosphenes evoked by all trials of

1078 sequence 4 (56, 58, 59, and 60). E. Average pattern of phosphenes evoked for each sequence tested.

1079 Patterns have been vertically displaced to allow easier comparison. Scale bar indicates 1°. F. Separation

1080 in visual space between phosphenes associated with particular electrode pairs as they appear in different
1081 sequences. The colored circles represent the pair of phosphenes for which the distance measurements
1082 were taken. For example, the first set of bars indicates the separation in visual space for phosphenes
1083 evoked by electrodes 56 and 58. This pair was measured in sequences 1, 2, and 4. In the case of patterns
1084 1 and 2, there was an intermediary electrode (57) presented between 56 and 58, the distance in both cases
1085 was 3.8° , whereas when stimulation was delivered to 56 and 58 consecutively, the distance between the
1086 resulting phosphenes was 1.6° .
1087



1088

1089 Figure 10. Comparison of overall map of visual space obtained by absolute mapping and visual space

1090 map fit to relative mapping with multi-point data. A. Array placement on the medial wall for BS1.

1091 Electrode 1 is indicated in the superior - anterior position, and electrode 60 in the inferior posterior

1092 direction. B. BS1 phosphene map generated by absolute mapping. C. BS1 visual filed map made by

1093 fitting a model of the V1-V3 complex to phosphene locations determined through relative multi-point

1094 mapping. D. Array placement for BS2. E. BS2 absolute phosphene map. F. BS2 visual field map

1095 generated by fitting a model of the V1-V3 complex to multi-point sequence data.

1096

1097

1098

1099

1100

1101

1102

1103

1104

1105

1106

1107

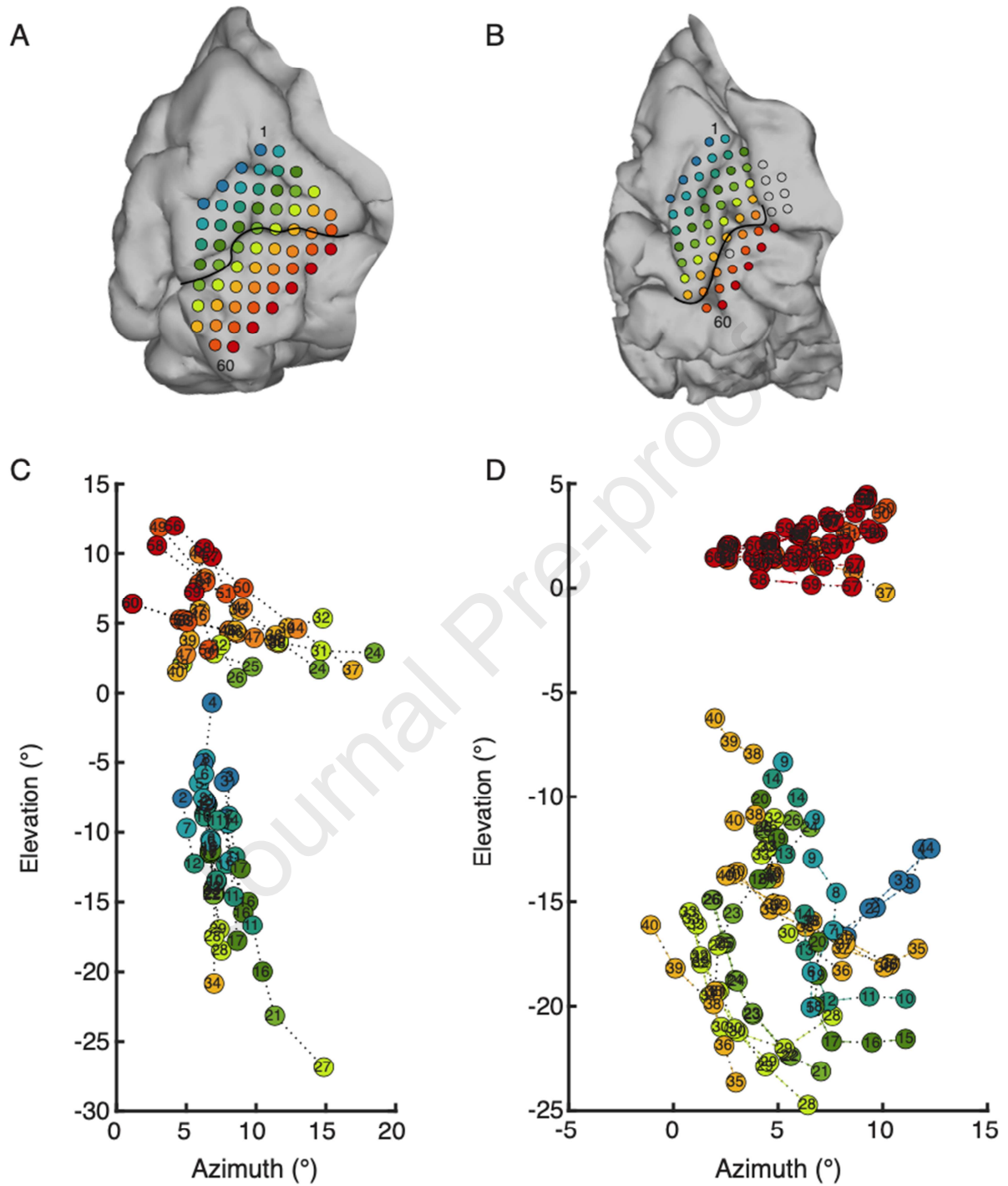
1108

1109

1110

1111

1112



1113

1114 Figure S1. All multi-point sequences collected for BS1 and BS2. A. Array placement for BS1. B. Array

1115 placement for BS2. Grayed out electrodes indicate electrodes that were placed outside of early visual

1116 cortex or were not functional. C. Phosphene patterns evoked by all multi-point sequences tested for BS1.

1117 D. Phosphene patterns evoked by multi-point sequences for BS2.

1118

1119

1120

1121

1122

1123

1124

1125

1126

1127

1128

1129

1130

1131

1132

1133

1134

1135

1136

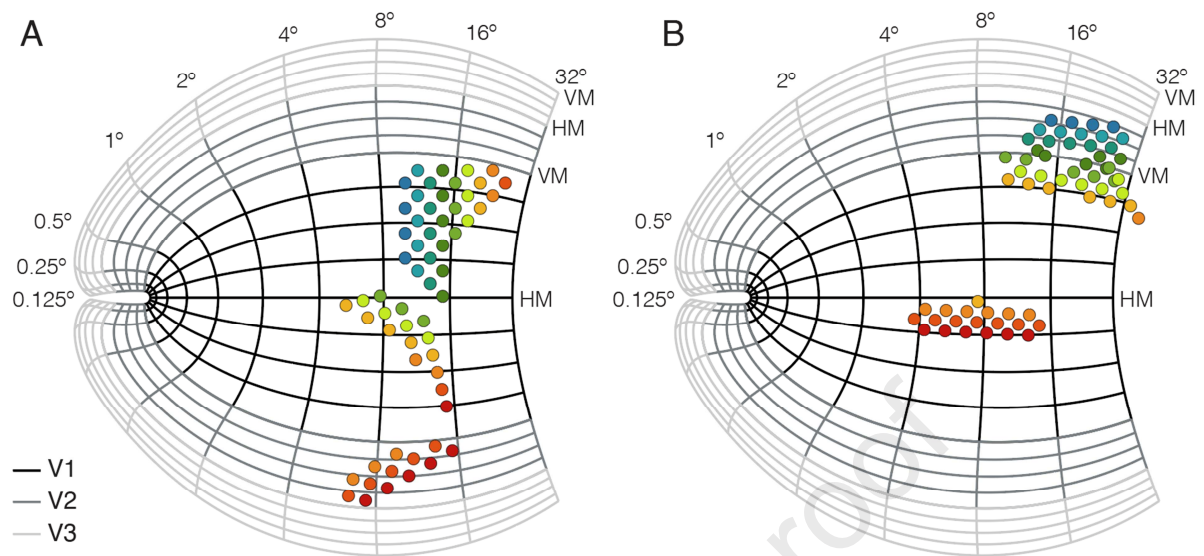
1137

1138

1139

1140

1141



1142

1143 Figure S2. Fit of model of V1 – V3 complex (Banded Double-Sech) to relative mapping data for BS1 and

1144 BS2. A. Flat map of the cortical sheet for BS1 with best fit location of implanted array. Exact array

1145 placement was determined by a cost function minimizing the weighted distance between cortical

1146 projections of reported phosphene location collected with multi-point mapping and the location of the

1147 electrodes that evoked each phosphene within the rigid structure of the array. The array was divided into

1148 three segments that were separately fit to either side of the calcarine fissure in each visual area (V1, V2).

1149 Dark grey lines indicate iso-azimuth and iso-elevation lines in V1, the medium gray lines indicate V2, and

1150 light gray indicates V3. This array placement was used to determine the phosphene map for BS1

1151 presented in Figure 10C. B. Flat map of cortical sheet of early visual cortex for BS2 with array placement

1152 derived in the same manner as BS1. This array placement was used to determine the phosphene map for

1153 BS1 presented in Figure 10F.

1154

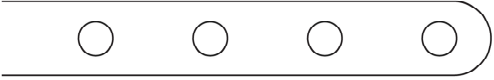

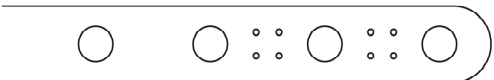

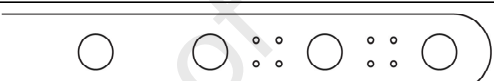
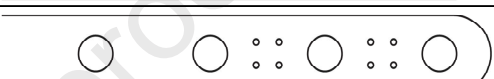
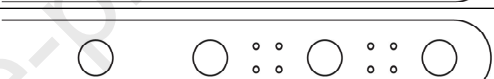
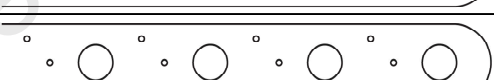
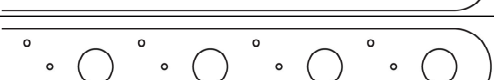






1155

1156

1157

1158

1159

| Global ID | Local ID | No. Macros | No. Minis | Strip Layout |
|-----------|----------|------------|-----------|--------------------------------------------------------------------------------------|
| LF | SS1 | 8 | 0 |  |
| MR | SS2 | 8 | 0 |  |
| YAA | SS3 | 8 | 8 |  |
| YAB | SS4 | 8 | 8 |  |
| YAC | SS5 | 8 | 8 |  |
| YAE | SS6 | 8 | 8 |  |
| YAF | SS7 | 8 | 8 |  |
| YAH | SS8 | 8 | 12 |  |
| YAI | SS9 | 8 | 12 |  |
| YAM | SS10 | 8 | 12 |  |
| YAN | SS11 | 8 | 12 |  |
| YAO | SS12 | 8 | 12 |  |
| YAU | SS13 | 8 | 16 |  |
| YAV | SS14 | 8 | 16 |  |
| YAX | SS15 | 8 | 16 |  |

1160

1161 Table S1. Sighted subject array information. Table indicates sighted subject global and local identifiers,

1162 the number of macro and mini electrodes implanted, and the electrode layout of the strip implanted. Large

1163 circles indicate locations of 3 mm clinical recording electrodes, small circles indicate 0.5 mm mini
1164 electrodes used for research purposes.

Journal Pre-proof

- Blind participants have difficulty reliably localizing phosphenes evoked by electrical stimulation of early visual cortex
- Bimanual fixation improves precision of reported phosphene location
- Relative mapping with multi-electrode sequences improves precision of reported phosphene location
- The spatial configurations of phosphenes observed during electrical stimulation of multi-electrode sequences is stable across trials
- Fitting a map model of the V1 – V3 complex to multi-point sequence data can be used to make an overall estimate of the visual field map of early visual cortex in blind subjects

Journal Pre-proof